

The Contact Metamorphic Effects of a Granitoid Pluton
On Zinc-Lead Mineralization in the Manganiferous
Metasediments of the Meguma Group, Eastville,
Colchester County, Nova Scotia

Submitted by

Barry Cameron

March 8, 1985

In partial fulfillment for a Bachelor of
Science Honours Degree,
Dalhousie University, Halifax, Nova Scotia

Distribution License

DalSpace requires agreement to this non-exclusive distribution license before your item can appear on DalSpace.

NON-EXCLUSIVE DISTRIBUTION LICENSE

You (the author(s) or copyright owner) grant to Dalhousie University the non-exclusive right to reproduce and distribute your submission worldwide in any medium.

You agree that Dalhousie University may, without changing the content, reformat the submission for the purpose of preservation.

You also agree that Dalhousie University may keep more than one copy of this submission for purposes of security, back-up and preservation.

You agree that the submission is your original work, and that you have the right to grant the rights contained in this license. You also agree that your submission does not, to the best of your knowledge, infringe upon anyone's copyright.

If the submission contains material for which you do not hold copyright, you agree that you have obtained the unrestricted permission of the copyright owner to grant Dalhousie University the rights required by this license, and that such third-party owned material is clearly identified and acknowledged within the text or content of the submission.

If the submission is based upon work that has been sponsored or supported by an agency or organization other than Dalhousie University, you assert that you have fulfilled any right of review or other obligations required by such contract or agreement.

Dalhousie University will clearly identify your name(s) as the author(s) or owner(s) of the submission, and will not make any alteration to the content of the files that you have submitted.

If you have questions regarding this license please contact the repository manager at dalspace@dal.ca.

Grant the distribution license by signing and dating below.

Name of signatory

Date



DALHOUSIE UNIVERSITY

Department of Geology

Halifax, N.S. Canada B3H 3J5

Telephone (902) 424-2358 Telex: 019-21863

DALHOUSIE UNIVERSITY, DEPARTMENT OF GEOLOGY

B.Sc. HONOURS THESIS

Author: Barry Cameron

Title: "The Contact Metamorphic Effects of a Granitoid Pluton On Zinc-Lead Mineralization in the Manganiferous Metasediments of the Meguma Group, Eastville, Colchester County, Nova Scotia".

Permission is herewith granted to the Department of Geology, Dalhousie University to circulate and have copied for non-commercial purposes, at its discretion, the above title at the request of individuals or institutions. The quotation of data or conclusions in this thesis within 5 years of the date of completion is prohibited without permission of the Department of Geology, Dalhousie University, or the author.

The author reserves other publication rights, and neither the thesis nor extensive extracts from it may be printed or otherwise reproduced without the authors written permission.

Signature of author

Date: April 4, 1985

COPYRIGHT

Table of Contents

	Page
List of Figures	iii
List of Tables	iv
Abstract	v
Acknowledgements	vi
Chapter 1 : Introduction	
1.1 General Statement	1
1.2 Location	3
1.3 Previous Work	5
1.4 Purpose and Scope	10
1.5 Methods and Approach	11
1.6 Organization	13
Chapter 2 : Geology	
2.1 Regional Geology	15
2.1.1 The Meguma Group	
2.1.1a Stratigraphy	15
2.1.1b Intrusive Rocks	19
2.1.1c Structure	20
2.1.1d Metamorphism	22
2.1.2 The Windsor Group	24
2.2 Local Geology	
2.2.1 General Statement	24
2.3 The Eastville Deposit	
2.3.1 General Statement	25
2.3.2 Domain I - Regional Metamorphic	
2.3.2a Stratigraphy	28
2.3.2b Structure	28
2.3.2c Petrography	29
2.3.3 Domain II - Granitoid Pluton	31
2.3.4 Domain III - Contact Metamorphic	
2.3.4a Stratigraphy	35
2.3.4b Structure	36
2.3.4c Petrography	37
2.4 Glacial Deposits	42
2.5 Summation	43
Chapter 3 : Trace Element Geochemistry	
3.1 Igneous Rocks	45
3.1.1 Trace Element Study of Granitoid Pluton	45
3.2 Meguma Group Rocks	53
3.2.1 Trace Element Study of the Meguma Group	54
3.3 Summation	58
Chapter 4 : Mineral Analyses	
4.1 General Statement	59
4.2 Minerals	
4.2.1a Garnet in the Meguma Group	59
4.2.1b Garnet in the Granitoid	60
4.2.2 Biotite	65
4.2.3 Chlorite	68
4.2.4 White Mica	70
4.2.5 Oxide Needles	71
4.2.6 Staurolite	72

4.2.7 Andalusite	73
4.2.8 Plagioclase in the Granitoid	74
4.3 Discussion	74
Chapter 5 : Pressure-Temperature Conditions	
5.1 General Statement	78
5.2 Mineral Assemblages	
5.2.1 Regional Metamorphic Conditions	78
5.2.2 Contact Metamorphic Conditions	79
5.3 Garnet-Biotite Geothermometry	80
Chapter 6 : General Discussion	
6.1 Relative Age of the Mineralization	83
6.2 Metamorphism at Eastville	85
6.3 Late Remobilization	86
6.4 Interaction of Rock Types	87
Chapter 7 : Conclusions	90
Chapter 8 : Recommendations	92
References	93
Appendix 1 - Trace Element Data for Granitoid	97
Appendix 2 - Trace Element Data of Hole 26	98
Appendix 3 - Major Element Data for Granitoid	101
Appendix 4 - Major Element Data for Hole 26	102
Sample Location - Drill Hole 26	104

List of Figures

	Page
Chapter 1 : Introduction	
Figure 1.1 Metallogenic Map	2
Figure 1.2 Study Area Location Map	4
Figure 1.3 AFMAG Anomaly	6
Figure 1.4 Drill Hole Location	8-9
Figure 1.5 Sample Location	12
Chapter 2 : Geology	
Figure 2.1 Geology of the Meguma Zone	16
Figure 2.2 Structural Map of the Meguma Zone	21
Figure 2.3 Local Geology Map and Domain Divisions	26
Figure 2.4 Stratigraphy for Domain I	27
Figure 2.5 Garnet in the Granitoid	33
Figure 2.6 Garnet-Biotite Schist	39
Figure 2.7 Staurolite-Almandine Garnet-Biotite Schist	39
Chapter 3 : Trace Element Geochemistry	
Figure 3.1 Ba vs. Rb Granitoid Plot	47
Figure 3.2 Zr vs. TiO ₂ Granitoid Plot	47
Figure 3.3 Rb-Sr-Ba Granitoid Triangular Diagram	49
Figure 3.4 Rb-Ba-Zr Granitoid Triangular Diagram	50
Figure 3.5 Rb-Sr-Zr Granitoid Triangular Diagram	51
Figure 3.6 Pb-Zn-Cu Granitoid Triangular Diagram	52
Figure 3.7 Rb-Sr-Ba Hole 26 Triangular Diagram	55
Figure 3.8 Rb-Sr-Zr Hole 26 Triangular Diagram	56
Figure 3.9 Pb-Zn-Cu Hole 26 Triangular Diagram	57
Chapter 4 : Mineral Analyses	
Figure 4.1 Granitoid Garnet Profiles	62-63
Figure 4.2 (FeO+MnO)-MgO-TiO ₂ Biotite Triangular Plot	67

List of Tables

	Page
Chapter 3 : Trace Element Geochemistry	
Table 3.1 Mean Trace Element Content of Granodiorite	46
Chapter 4 : Mineral Analyses	
Table 4.1a Chemical Trends in Metamorphic Garnets	60
Table 4.1b Meguma Group Garnet Compositions	64
Table 4.1c Granitoid Garnet Compositions	64
Table 4.1d Garnet Profile Compositions	65
Table 4.2a Biotite in Granitoid Compositions	66
Table 4.2b Biotite Compositions in Meguma Group	68
Table 4.2c Chemical Trends in Biotite	68
Table 4.3a Chlorite Compositions	70
Table 4.3b Chemical Trends in Chlorite	70
Table 4.4 White Mica Compositions	71
Table 4.5 Oxide Needles Composition	72
Table 4.6 Staurolite Composition	73
Table 4.7 Andalusite Composition	74
Table 4.8 Plagioclase Composition in the Granitoid	74
Chapter 5 : Pressure-Temperature Conditions	
Table 5.1 Geothermometry Data	81

Abstract

The Contact Metamorphic Effects of a Granitoid Pluton on Zinc-Lead Mineralization in the Manganiferous Metasediments of the Meguma Group, Eastville, Colchester County, Nova Scotia

The distribution of mineral resources in the Meguma Zone has been found to be spatially associated with the transition of the Goldenville and Halifax Formations (GHT, Zentilli and MacInnis, 1984). The Eastville deposit constitutes the only significant zinc and lead mineralization in the Cambro-Ordovician Meguma rocks. The study area is located between Eastville and Hattie Lake, Colchester County, and consists of a 10 km section of steeply dipping GHT, striking to the northeast. The deposit is intruded by a Devonian-Carboniferous granitoid pluton making this locality a unique place to study the interaction of granitoids with mineralized GHT.

The boundary between the Goldenville and Halifax Formations can be mapped by the presence of a locally calcareous and contorted manganiferous bed consisting of intercalations of quartz metawacke and slate. The Meguma Group of the Eastville area has undergone regional metamorphism to lower greenschist facies reflected in the observed assemblage of chlorite + spessartine garnet + muscovite + quartz, indicating temperatures of between 370 and 420°C. Heat from the intrusion of the granitoid pluton thermally metamorphosed the country rock to a staurolite-almandine garnet-biotite schist. Garnet-biotite geothermometry has been used to estimate the temperature of this episode at around 580°C, which agrees well with mineral assemblage estimates. The contact aureole is distinct by the absence of carbonate. The granitoid pluton at Eastville is a peraluminous granodiorite-monzogranite complex that can be interpreted as being produced by magmatic differentiation. The biotite granodiorite contains reversely zoned garnets as an accessory mineral.

Sphalerite in the cores of some regional metamorphic spessartine garnet indicates the Zn mineralization is of pre-regional metamorphic age. This textural evidence poses constraints on possible genetic hypotheses. The relatively old age of the mineralization and the complex history of the Meguma Zone has increased the probability of post-depositional redistribution of the base metals.

Acknowledgements

I would like to thank Dr. Marcos Zentilli for suggesting this thesis project. His enthusiasm and ability to coordinate a team effort has been largely responsible for any amount of success achieved by the Economic Geology Research Group. I would also like to thank my colleagues in the Economic Geology Research Group, Ian MacInnis and Robert Hingston, for sharing work space and providing guidance through any problems encountered in this research. I appreciate Casey Ravenhurst's assistance, who lended a hand even though his project was not directly related to mine. Mr. Robert MacKay provided expert assistance in the microprobe analyses. I thank Ms. Sharon Frail for her understanding and interest shown in my thesis. I would especially like to recognize the contribution of my mother and father, Anne and Chester Cameron, in the completion of this thesis. Their support through the years of my education is very much appreciated. Research was financed through grant A-9036 to M. Zentilli from the Natural Sciences and Engineering Research Council (NSERC) of Canada.

CHAPTER 1 : Introduction

1.1 General Statement

When one views a geological map of Nova Scotia an obvious pattern of mineral resource distribution is evident in the Meguma Zone. Figure 1.1 shows the location of some mineral occurrences in relation to the bedrock geology of a section of central Nova Scotia. The majority of economic and sub-economic mineral concentrations of tungsten, gold, antimony, and arsenic in the Meguma Zone have been found to be spatially associated with the transition between the Goldenville and Halifax Formations (henceforth GHT, Zentilli and MacInnis, 1984). The Eastville deposit constitutes the only significant zinc and lead mineralization in the Cambro-Ordovician Meguma Group. Sulpetro Mines Ltd. of Truro, previously St. Joseph Explorations Ltd., owns the claims covering the Eastville deposit. It should not be surprising that the Eastville deposit also is found in the GHT, and therefore is of great importance in the understanding of the metallogeny of this transition.

The Eastville deposit consists of a 10 km section of steeply dipping GHT striking to the northeast, and is truncated in the east by a monzogranite-granodiorite pluton. The purpose of this thesis is to understand the effects of the above pluton on the deposit and its host rocks from the point of view of metamorphic petrology and geochemistry.

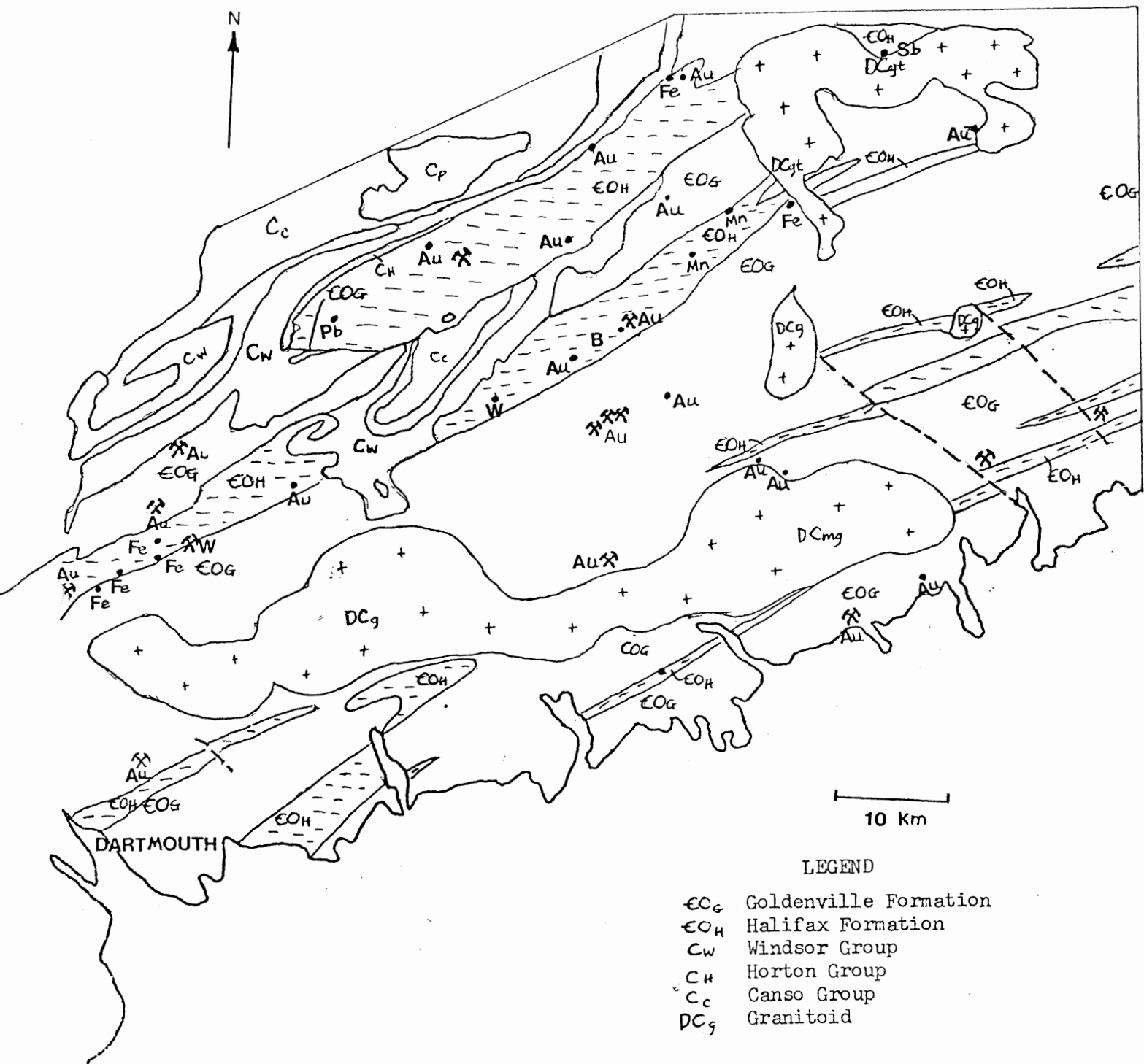


FIGURE 1.1 Note the spatial association between the transition of the Halifax and Goldenville Formations and mineral occurrences in Nova Scotia.

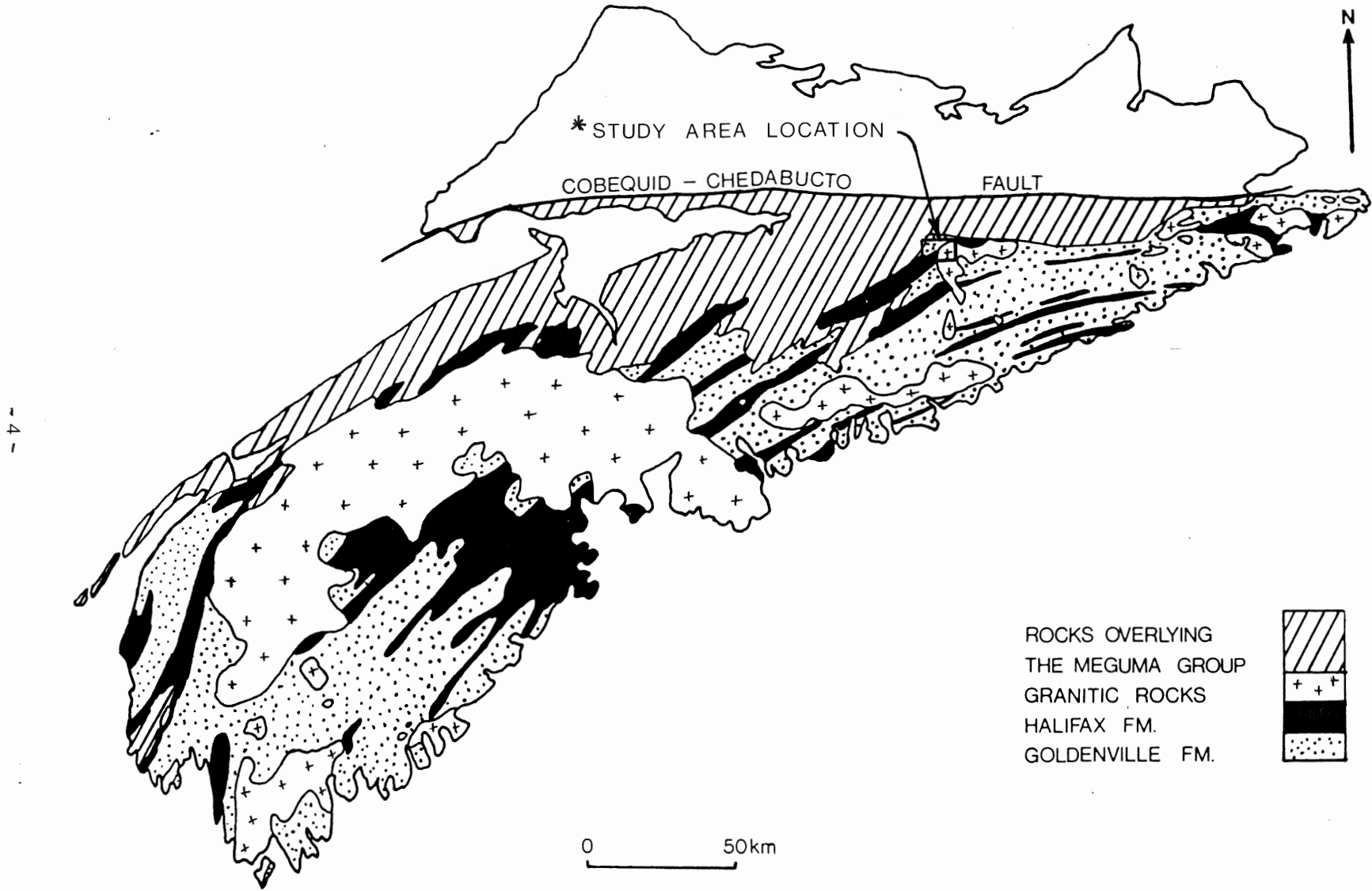
The importance of the Eastville deposit is immense in view of suggestions that the source of Pb in the carbonate-hosted deposits of the Carboniferous Basin is the Meguma basement.

1.2 Location

Eastville is located in Colchester County, about 40 km southeast of Truro, Nova Scotia (Figure 1. 2). The Eastville deposit covers the area from $45^{\circ}15'30''$ latitude, $62^{\circ}52'30''$ longitude to $45^{\circ}17'45''$ latitude, $62^{\circ}44'30''$ longitude in NTS topographic sheet 11E7. Eastville may be reached from Halifax through Route 102 taking Exit 12 to Brookfield, where Route 289 E is followed to Springside Cross Road. A right turn at this Cross Road, followed by a left at the next intersection leads to the town of Eastville. At Eastville right turns onto Harrison and Fisher Roads leads to the Eastville Road, a good quality gravel road, which provides access to the deposit, and leads to Trafalgar 19 km to the east. A network of logging roads belonging to Scott Paper cover much of the property, but are less reliable and may only permit entrance by truck or foot.

The topography of the Eastville area varies from the western to eastern sections of the deposit. In the west, the terrain is irregular and hummocky, while in the east the topography is more gentle. In this more gentle eastern section, breaks in topography can be attributed to the presence of faults. The study area is densely forested, and

FIGURE 1.2 Study Area Location Map



is presently being worked by Scott Paper. Lakes are quite abundant around Eastville , while the drainage is poor with Cox Brook being the only large flowing river in the vicinity. Glacial overburden tends to be thick in this region ranging from 0 to 10 m, with the average falling close to 10 m. Outcrops are scarce.

1.3 Previous Work

The Eastville area was first mapped at a scale of 1:63,360 by H. Fletcher and E.R. Faribault (1902), who were mainly interested in mineral showings and structure. The area was remapped by D.G. Benson (1967). He modified Fletcher and Faribault's map, and ascribed (erroneously) much of the rock to the southeast of Eastville to part of the Goldenville Formation. Most recently Binney et al.(1985) has confirmed and extended much of Fletcher and Faribault's early mapping. He used the logging roads, extensive diamond drilling and surface geophysics to map the area at a scale of 1:10,000.

While exploring for gold in 1976, St. Joseph Explorations Limited noticed a significant northeast-trending electromagnetic anomaly (Figure 1.3). Soil sampling was carried out, and analysis outlined a westward-trending lead anomaly with Pb values greater than 1,000 ppm. The anomaly was coincident with the contact of the Goldenville and Halifax Formations. Initially three

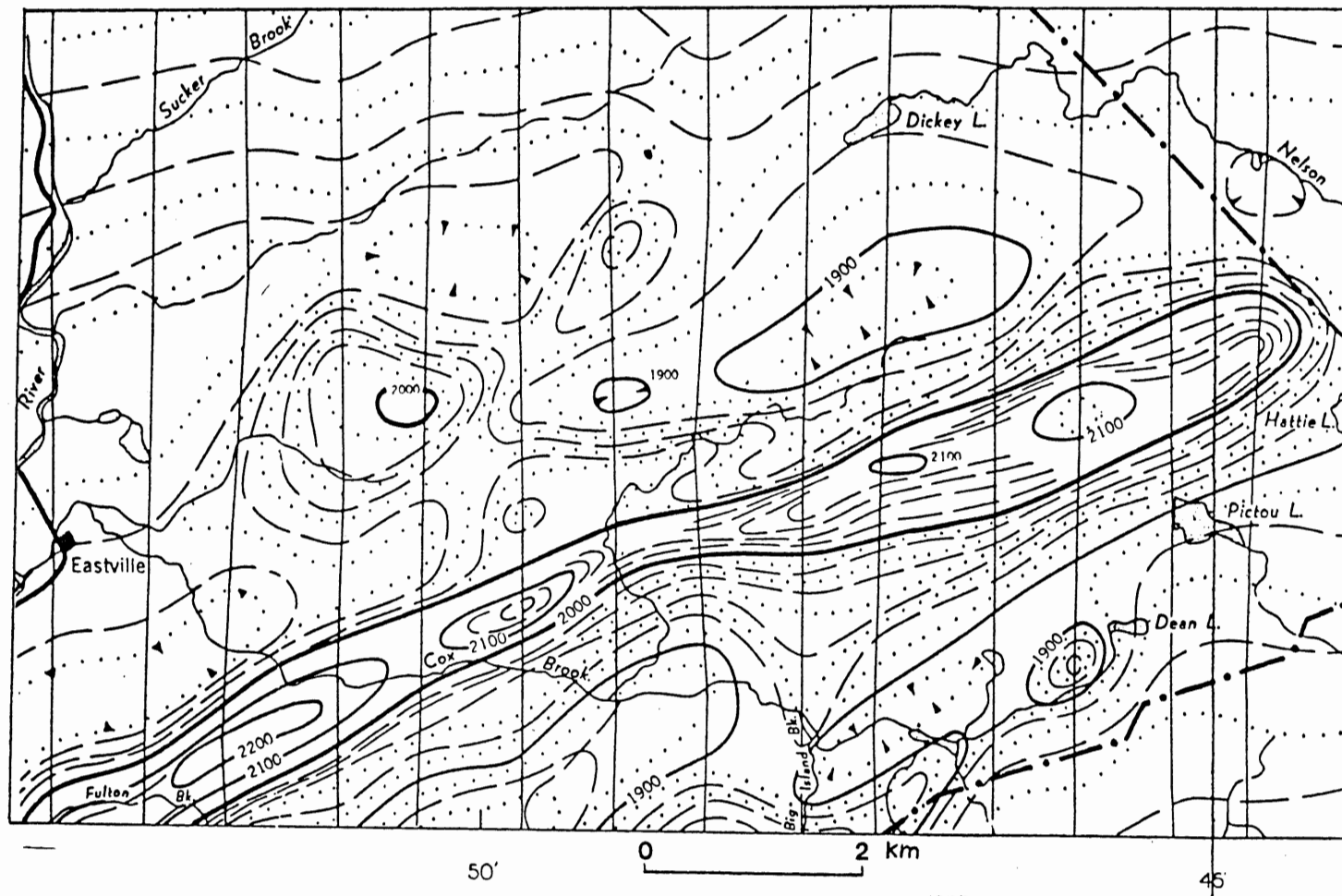


FIGURE 1.3 Electromagnetic anomaly in the Eastville area which led to St. Joseph Explorations Limited's interest in the property. The anomaly trends northeast and is 200 gammas above background. (taken from GSC Aeromagnetic map 762G)

diamond drill holes established the presence of mineralization in the form of fine grained sphalerite and galena. Grids were then cut following the major geochemical anomalies. Twenty-eight diamond drill holes in total have been used to investigate the extent of the deposit (Figure 1.4).

The exploration so far has not outlined an economic grade and tonnage of zinc and lead. On average, the drill holes include 2 m to 10 m sections of 1 to 3 percent combined zinc-lead. Of more importance are hole 7, which contains 3.34 percent combined zinc-lead over 6.1 m of black slate, and hole 28, which has 4.09 percent combined zinc-lead over 9.33 m in fault gouge at the contact between the Goldenville and Halifax Formations (Binney et al,1985).

Interest in the Eastville property has grown, with many studies investigating various aspects of the deposit. Jenner (1982) described the styles of mineralization and associated lithologies. She interpreted the coexistence of chlorite and biotite in the metasedimentary rocks to indicate metamorphism of middle greenschist facies. MacInnis (1983) conducted a geochemical study of the manganiferous metasedimentary rocks of the Goldenville-Halifax contact at Eastville. MacInnis (1984) furthered his study to include carbon and oxygen isotope data on carbonate concentrations in the Meguma rocks at Eastville. He concluded that the carbonate resulted from

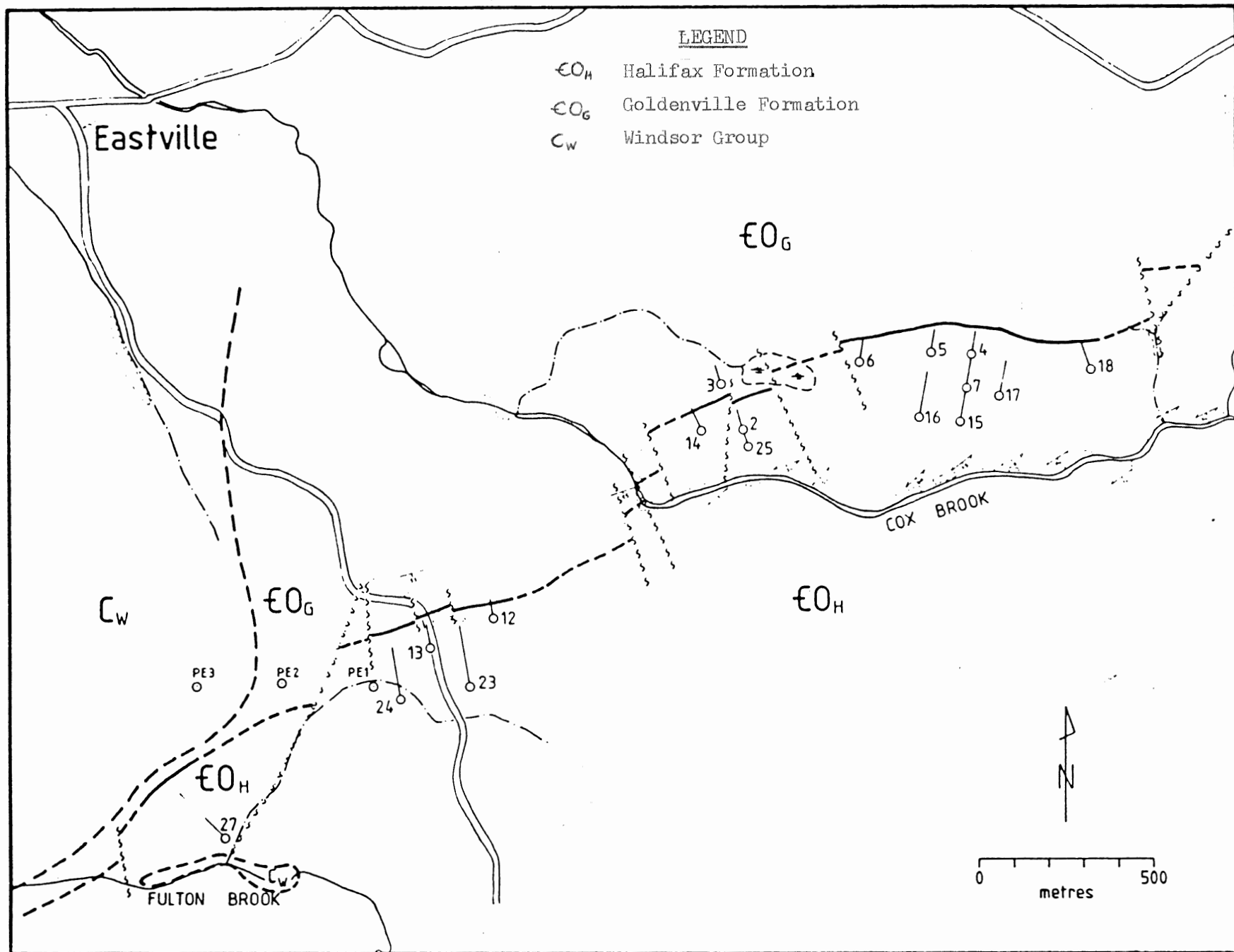


FIGURE 1.4 Drill Hole Location Map of the Western Section

LEGEND

- €O_H Halifax Formation
- €O_{HA} Contact Aureole
- €O_G Goldenville Formation
- DC_G Granitoid

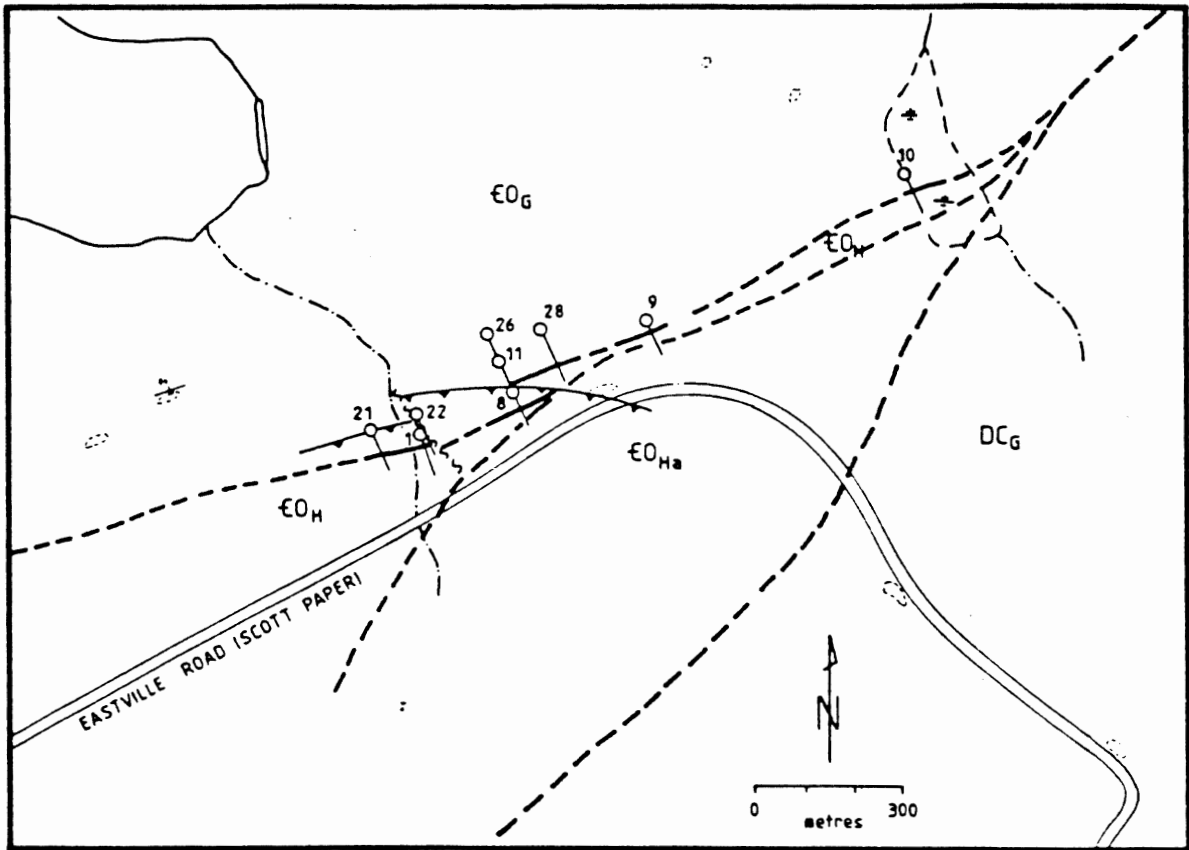


FIGURE 1.4 (Continued) Drill Hole Location Map of the Eastern Section
(from Binney et al., 1985)

oxidation of organic matter. No work had been done to investigate the effect of the granite on Zn-Pb mineralization in the metasedimentary country rock.

1.4 Purpose and Scope

The fundamental purpose of this thesis is to determine the relative age of the zinc-lead mineralization at Eastville with respect to the metamorphic and intrusive events. Petrographic description of the minerals and textures of the rocks should aid in this determination. Many questions are addressed in an attempt to understand the role of metamorphism and igneous activity on the geology of the study area : 1) What are the mineralogical-geochemical effects of the pluton on the different lithologies as it is approached from the west? 2) Can one obtain an estimate of the temperature of metamorphism from the polymetamorphic assemblages? 3) Is there any evidence for assimilation, and if so, what are the effects of the distinct lithologies on the pluton itself? 4) How does the pluton in the eastern section of Eastville compare with other granitoids in the region?

It is not in the scope of this thesis to actually suggest models for the genesis of the Eastville deposit, although the findings of this study do provide a clearer picture of the models which warrant merit. Time limitations do not allow for an extensive geochemical study of the

pluton, but rather should establish a baseline for further studies.

1.5 Methods and Approach

Field work in the study area was conducted to map the contact between the granitoid and Meguma rocks, and to collect specimens of the granitoid. The location of the granitoid samples are shown in Figure 1.5. Core from the twenty-eight drill holes provided an abundance of samples of Meguma metasedimentary rock but, because the core never intersected the granitoid, field work was necessary to obtain samples of the intrusive rocks.

Field work was done on four separate occasions, three trips occurring in the summer of 1984, and the fourth was taken in the fall. The first trip taken early in the summer was used to gain a better understanding of the regional and local geology. On June 23 and 24, three samples were collected, and magnetic traverses were run to be used in mapping contacts between the rock units. The day of August 18 was spent collecting 6 granitoid and three Meguma rock specimens, and mapping the contact along Cox Brook. Finally October 13 was used to collect samples and study the structure of a manganiferous, contorted bed in outcrop, and to confirm the contact between the granite and Meguma rock south of Cox Brook.

Twenty thin sections were prepared from the granitoid

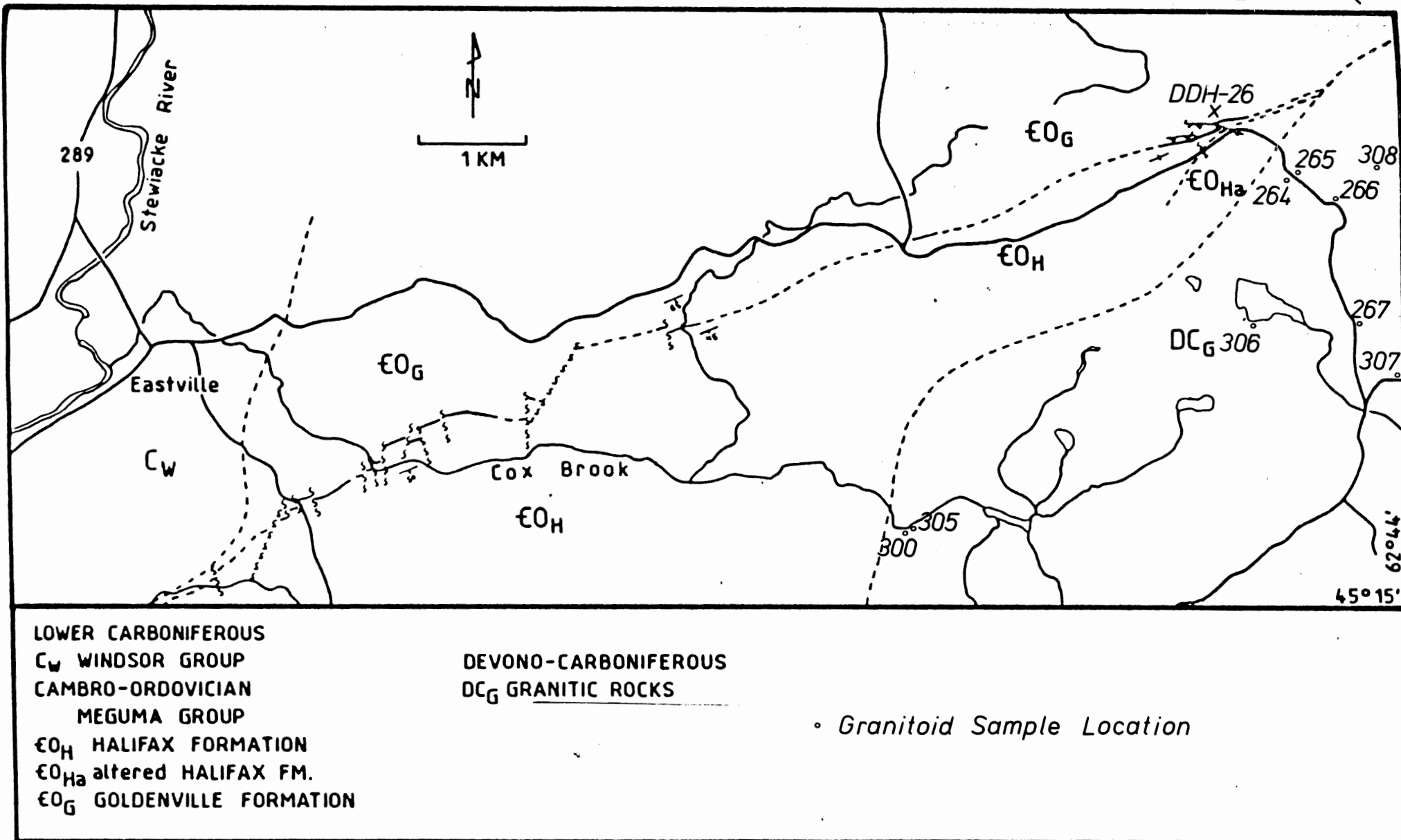


Figure 1.5 GRANITOID SAMPLE LOCATION MAP

specimens to study the mineralogy and textures of the intrusive body. One polished thin section of a granitoid was made. Ninety-six polished and eighty-two normal thin sections were available of the Meguma Group rocks at Eastville as part of a more regional study into the GHT. From this collection, twenty thin sections that were thought to be representative of the various lithologies were described in detail.

Microprobe analysis of polished thin sections was performed to obtain the chemical composition of some important metamorphic minerals. The granitoid polished thin section was probed for garnet zoning. Powdered samples of the granitoid specimens and of drill hole 26 were sent to St. Mary's University's XRF lab for major and trace element analysis. Only the trace element results have been received at the time of first printing.

1.6 Organization

The thesis has been organized into eight chapters. The first chapter has been used to introduce the study area, and describe the approach that will be taken to achieve the purposes set out. Chapter 2 involves a detailed discussion of the regional geology as it pertains to this thesis, and moves on to a description of the geology of the Eastville area. Full understanding of the rock types would not be possible without their chemical compositions, which is dealt

with in Chapter 3. A natural progression from the study of the rocks is an investigation into the chemical composition of the mineral phases. Chapter 4 includes chemical data from microprobe analyses of a number of minerals, and a discussion of the results. Stability field diagrams and a garnet-biotite geothermometer are used in Chapter 5 to estimate the pressure-temperature conditions of the metamorphic events at Eastville. A general discussion of topics directly related to the outlined purposes occurs in Chapter 6. The conclusions of this study are presented in Chapter 7, followed by a recommendation section in Chapter 8 which suggests questions requiring further work. Appendices 1 and 2 present the trace element data of the granitoid samples, and the Meguma rocks of Hole 26, respectively. Appendices 3 and 4 present the whole rock major element analysis of the same rocks.

CHAPTER 2 : Geology

2.1 Regional Geology

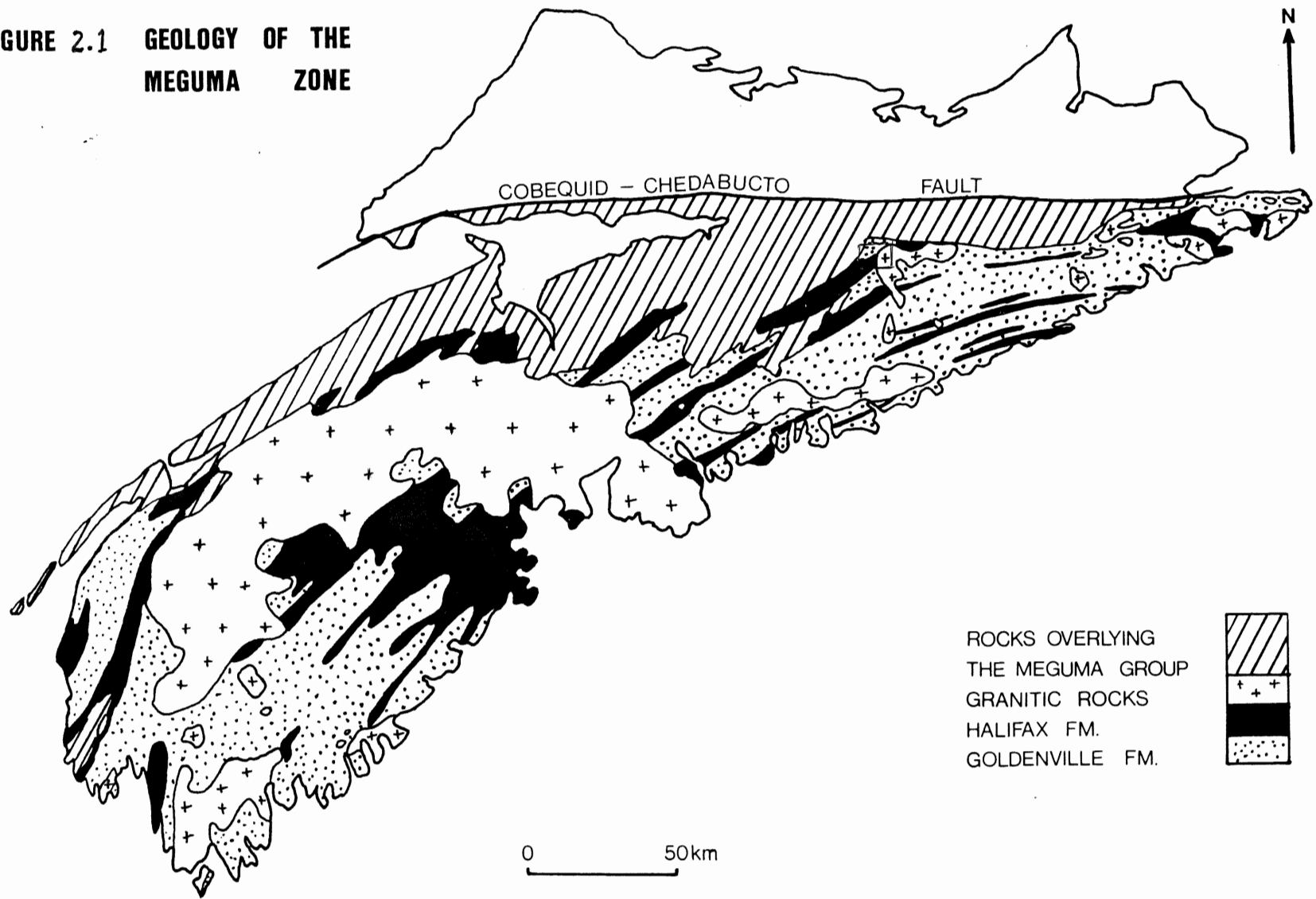
The Meguma Zone lies to the south of the Glooscap Fault in Nova Scotia. This zone exhibits both lithological and deformational contrasts to the adjacent Avalon Zone. The geology of the Meguma Zone is shown in Figure 2.1. The Meguma Zone consists of a thickness of more than 14 km of Cambrian to Devonian metasedimentary rocks with minor metavolcanic units. This sequence was metamorphosed during the Acadian Orogeny, and later intruded by Devonian batholiths. Lower Paleozoic sedimentary rocks of the Meguma Zone are a conformable sequence of interstratified black slates and metaquartzites of eugeosynclinal-flyschoid facies (Schenk, 1970).

2.1.1 The Meguma Group

2.1.1a Stratigraphy

The Meguma Group rocks are the oldest exposed rocks of southwestern Nova Scotia, and may exceed 10 km in thickness. This group forms both the bedrock for most of the Meguma Zone, and the foundation of the offshore Scotian Shelf, a total area of about 125,000 km² (Schenk, 1978). The Meguma Group consists of two formations, the basal Goldenville Formation and the overlying Halifax Formation. Schenk (1978) has interpreted the Meguma Group as a eugeoclinal

FIGURE 2.1 GEOLOGY OF THE MEGUMA ZONE



complex of a deep sea fan and overlying continental rise. Paleocurrent directions indicate the source of the Meguma Group sediments was a granitic craton to the south and east (Schenk,1970).

The Goldenville Formation consists of quartz-rich greywacke with interbeds of slate that increase in number and thickness towards the top of the sequence (Graves and Zentilli,1982). This formation tends to be thickly stratified displaying various primary sedimentary structures. These include parallel bedding,graded bedding, sole marks, crescent current ripples, cross stratification, contorted bedding,and convolute bedding (Taylor and Schiller,1968). These primary structures have contributed to the interpretation of deposition of the Meguma Group by turbidity currents. The greatest measured thickness of the Goldenville Formation is 5600 m, although the base has never been found exposed.

The Halifax Formation is composed predominantly of thinly laminated slates with interbedded siltstones and greywacke. The slates of this formation are often black owing to the presence of graphite. Secondary structures such as cleavage and joints are more important in the Halifax slates than primary structures. Only parallel bedding is common in the slates, while graded bedding, scour and fill structures, crossbedding, and ripple marks are rare. The Halifax Formation is about 4400 m thick in the

northwest, and thins to about 500m in the south (Schenk,1975b).

The boundary between the Halifax and Goldenville Formations is conformable, and Schenk has marked this transition by a ratio of metagreywacke to slate of one. More recently the widespread existence of a manganiferous zone in the upper section of the Goldenville Formation has been used to map the transition.

Limited paleontological data indicates the Meguma Group is of Cambro-Ordovician age. Slates of the Halifax Formation along the Bay of Fundy contain the graptolite Dictyonena flabelliforme, which assigns a minimum age of early Ordovician to the Meguma Group. Potassium argon ages of 476 ± 19 m.y. and 496 ± 20 m.y. have been obtained from detrital muscovite from the Goldenville Formation (Poole,1971). It is thought these ages reflect the time of deposition or diagenesis as they agree with the Arenigian age suggested by poorly preserved graptolites in the Goldenville Formation near Tangier Harbour. Dates for biotites from the Goldenville Formation of 338 m.y.(Fairbairn et al., 1968) and 383 m.y.(Lowdon et al.,1963) probably represent the time of regional metamorphism. Whole-rock slate data (Reynolds et al.,1973) places the age of the Acadian Orogeny between 400 and 415 m.y.

2.1.1b Intrusive Rocks

The Cambro-Ordovician Meguma Group is intruded by peraluminous granodiorite-monzogranite complexes. The largest of these granitoid intrusions in the Meguma Zone stretches from Halifax to Yarmouth, and forms the South Mountain. Individual plutons are abundant in Nova Scotia, and are found throughout the Meguma Zone. Reynolds et al.(1981) produced age dates of granitoid rocks from southern Nova Scotia which suggest a relatively simple history. Early and late phases of the granitoid plutons seem to have crystallized about 367 Ma ago. Clarke and Halliday (1980) used the Rb/Sr whole rock method for the South Mountain Batholith, and found a range of 361-372 Ma.

The plutons are granodiorite-monzogranite complexes in which biotite granodiorite is the dominant phase present (McKenzie and Clarke,1975). Metasedimentary xenoliths are quite abundant in the granodiorite. The xenoliths apparently were derived from the roof of the pluton as the existence of enclaves is not a function of proximity to external contacts (McKenzie and Clarke,1975). Apatite, zircon, opaque minerals and garnet may be present as accessory minerals.

Aplite and pegmatite dykes are found throughout the granitoid plutons of southern Nova Scotia. The dykes cut both the granodiorite and monzogranite phases indicating a

late magmatic stage. The distribution of the various phases of the granitoid has been explained by crystal-liquid fractionation involving the early separation of biotite and plagioclase. Clarke and Halliday (1980) showed the peraluminous magmas which formed the South Mountain Batholith were not derived by partial melting of the Meguma Group alone. They propose either partial melting at depth of a metasedimentary basement different from the Meguma, or the magmas are hybrids derived by melting of a composite source region.

2.1.1c Structure

Sediments in the Acadian geosyncline underwent three phases of Ordovician Taconian orogeny, while those in the Meguma Trough were unaffected until the Devonian Acadian orogeny (Schenk, 1970). The Meguma Group and other lower Paleozoic rocks of this zone have been affected by at least three generations of folds and faults (Fyson, 1966). Fyson's structural map is shown in Figure 2.2.

The main folds (F1) are upright, gently plunging with axial planes never inclined more than 20 degrees. The trend of the folds are northeast over much of southern Nova Scotia to east closer to Chedabucto Bay. The slates contain a slaty cleavage (S1) which is subparallel to the axial planes of these main folds. The trends of the folds are not disrupted where the granitoid plutons are intersected

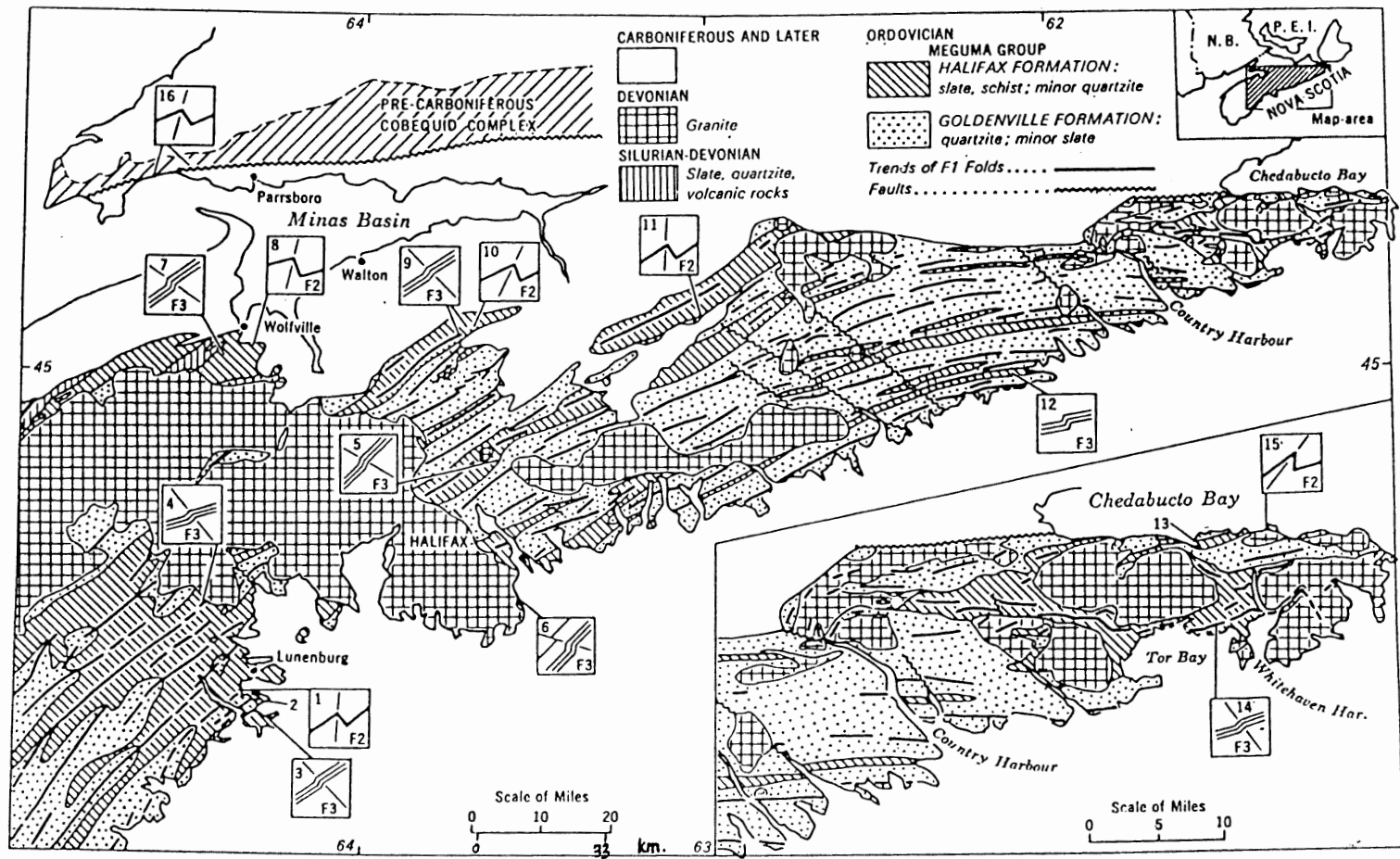


FIGURE 2.2 Structural Map of the Meguma Zone (Taken from Fyson, 1966)

(Fyson,1966).

Cross folds (F2 and F3) deform both the bedding (S0) and the axial plane cleavage (S1), which indicates a later stage of stress. Mesoscopic F2 folds are Z-shaped when viewed down plunge, and are considered interfolial. These Z-shaped folds are found within the metamorphic aureoles of the granitoid plutons. Unstrained andalusite porphyroblasts suggest the folds are older than the granitoid. The F3 fold structures are small S-shaped kinks in foliated rocks. These kinks deform porphyroblastic andalusite schists, and therefore indicate deformation was post contact metamorphism. Faults and fractures are related to F2 and F3 deformation.

2.1.1d Metamorphism

The intrusion of Devonian-Carboniferous granitoid has produced contact aureoles which overprint the regional metamorphic assemblages. The Meguma Group has been metamorphosed to the greenschist facies, and locally to the almandine-amphibolite facies (Taylor and Schiller,1968). Garnet, biotite and chlorite is a typical regional metamorphic assemblage in the Meguma Group, and suggest temperatures of 300-500°C and pressures of 3 to 5 kilobars. In the extreme south of Nova Scotia, the presence of staurolite and sillimanite elevates the grade to almandine-amphibolite facies of temperatures in the range of

550-750°C and pressures of 4 to 8 kb.

Rocks metamorphosed to greenschist facies are more susceptible to overprinting by contact metamorphism. The observed assemblages in contact aureoles indicate metamorphism to the hornblende-hornfels facies. Chiasolite, cordierite, staurolite, and sillimanite are characteristic contact metamorphic minerals. Temperatures of 550-700°C and pressures ($P_{H_2O}=P_{total}$) of between 1 and 3 kilobars are estimated for the contact metamorphism (Taylor and Schiller, 1968). The aureoles surrounding the intrusions are variable in extent due to the geometry of the contact.

Jamieson (1974) has shown the highest grades of thermal metamorphism should be achieved by xenoliths. These inclusions give a better indication of the temperature of the intrusion than the contact aureole rocks. Plagioclase, biotite and quartz occur in all xenoliths studied in the South Mountain Batholith, while garnet, cordierite, potassium feldspar, and sillimanite form with increasing grade. Jamieson (1974) determined that the majority of the xenoliths equilibrated at temperatures of 630 to 690°C and pressures of 3.1 to 3.5 kb, as yielded by the assemblage garnet+ cordierite+potassium feldspar+biotite+quartz. McKenzie and Clarke (1975) estimated temperatures of 650-700°C, and pressures of 3.3 to 4.0 kb for the emplacement of the South Mountain Batholith.

2.1.2 The Windsor Group

Strong uplift and erosion followed the Acadian orogeny and the intrusion of granitoid batholiths. Erosion over a period of about 12 million years exposed sections of the Meguma Group which had been buried several kilometres deep. Coarse to fine subaerial, fluvial to lacustrine siliclastic sediments were deposited in basins formed by the erosion of the Meguma basement. These siltstones and sandstones compose the Horton Group. This period of deposition was interrupted by marine sedimentation of carbonates, evaporites and red beds. The Windsor Group of middle to late Visean age consists of at least five cycles characterized by fossiliferous marine limestone and dolostone overlain by marine evaporites such as gypsum, anhydrite, halite, and minor potash, which was followed by siltstones and red beds (Akande and Zentilli, 1984). Carbonate banks occur only in areas where the Windsor Group oversteps the Horton Group to form on the granites and metasedimentary rocks comprising the basement. The basement ridge on which the Gays River carbonate bank formed includes the boundary between the Goldenville and Halifax Formations.

2.2 Local Geology

2.2.1 General Statement

The study area is dominated by the Meguma Group in the

northwest. The Eastville deposit consists of a steeply dipping, 10 km section of the transition between the Goldenville and Halifax Formations of the Meguma Group. The GHT strikes to the northeast. The deposit occurs on the northern limb of a tightly folded, upright syncline. Strike slip faults offset the transition in several areas, and a thrust fault exists in the eastern section of the deposit. In the southeast, the Meguma metasedimentary rocks are intruded by a granodiorite-monzogranite complex. Heat from the intrusion of this granitoid pluton produced a contact aureole in the adjacent Meguma rocks. Limestones, evaporites, and clastics of the Carboniferous Windsor Group unconformably overlie the Meguma rocks to the north and east.

2.3 The Eastville Deposit

2.3.1 General Statement

For the purpose of description, the study area has been divided into three domains. A domain is defined as an internally homogeneous geologic province with features that are in distinct contrast to those displayed in adjacent provinces. Accordingly the study area has been divided into a regional metamorphic domain (I), a granitoid domain (II), and a contact metamorphic domain (III). Figure 2.3 is a local geology map with the domain divisions shown.

2.2.2 Domain I - Regional Metamorphic Zone

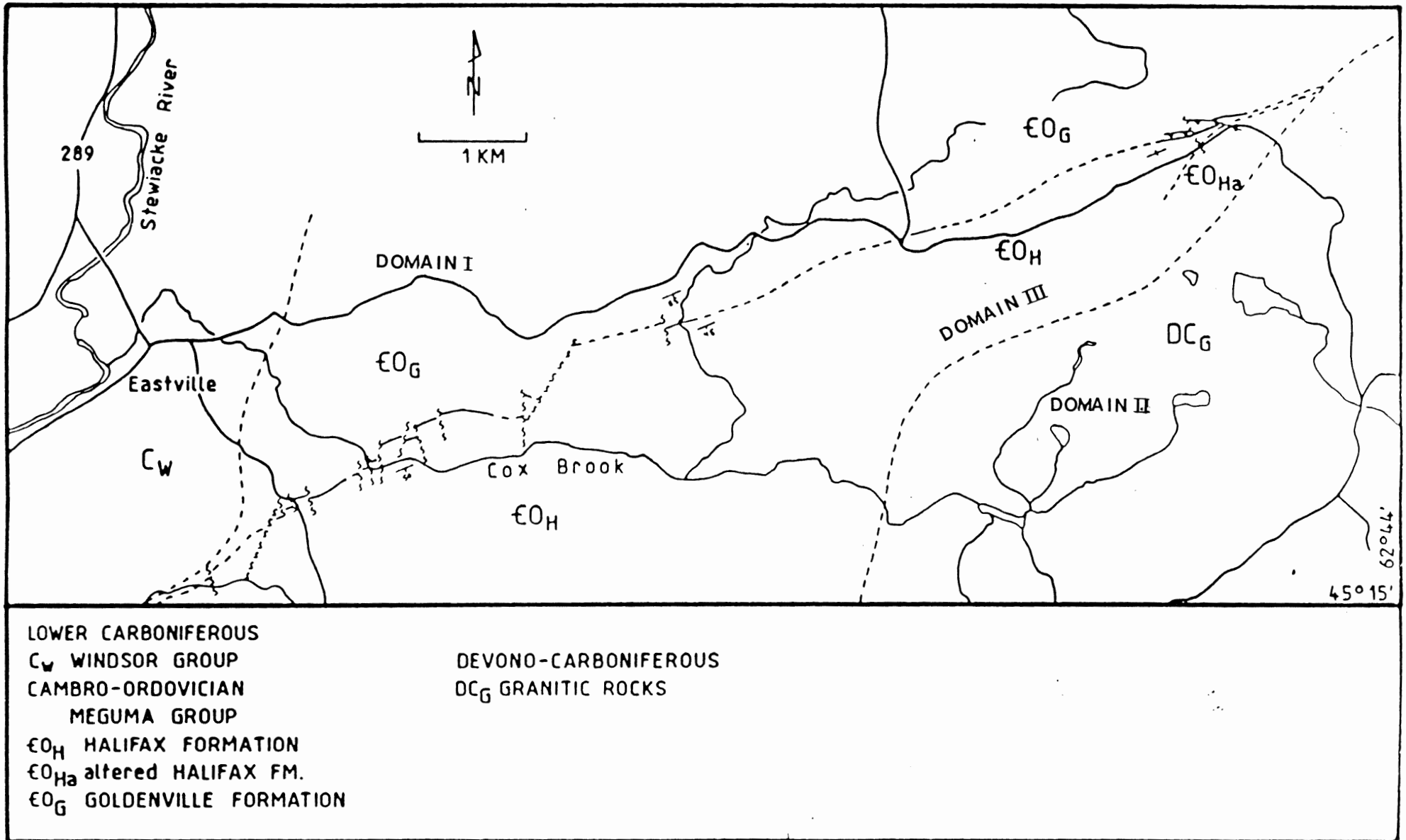


FIGURE 2.3 Local Geology Map showing the division into three domains.

		THICKNESS (metres)
HALIFAX FORMATION	BLACK SLATE AND FINE-LAMINATED TO CROSS-BEDDED QUARTZ WACKE.	+ 150
	CALCAREOUS QUARTZITE - THIN INTERBEDS OF QUARTZ WACKE, CALCAREOUS QUARTZ WACKE AND BLACK SLATE.	7-10
MEGUMA GROUP	TRANSITION ZONE - MASSIVE QUARTZ WACKE AND INTERBEDDED BLACK SLATE.	30-35
	GOLDENVILLE FORMATION	MASSIVE QUARTZ WACKE

FIGURE 2.4

Complete Stratigraphy of Domain I

(from MacInnis, 1983)

2.3.2a Stratigraphy

The regional metamorphic rocks in the western section of the deposit form a complete stratigraphic section. Drill core logs for holes from this domain distinguish four lithologies, and these are shown in Figure 2.4. Lithology 1 consists of a basal, massive quartz metawacke. At higher levels in the stratigraphic section interbeds of slate become increasingly more abundant. Lithology 2 begins where the preceding unit grades into interbeds of quartz metawacke and slate in about equal proportions, and is termed the Transition Zone. This zone grades upward into more finely laminated beds of quartz metawacke and slate still with a ratio of 1:1. This unit, Lithology 3, is characterized by its calcareous nature, severe contortions, and anomalous whole rock manganese contents. The contorted beds grade upward into Lithology 4, largely graphitic black slates of the Halifax Formation. Further upward in the section, grey-black slates occur with crossbedded to massive quartz metawacke interbeds.

2.3.2b Structure

Domain I forms part of the northern limb of a large northeasterly syncline in the Meguma Group deformed during the Devonian Acadian Orogeny. The deformation has placed the Goldenville Formation to the north of the Halifax Formation, which is to the south in the core of the

syncline. In outcrops along Cox Brook, the conformable Halifax and Goldenville Formations have been found to dip to the south at 55 to 75 degrees. Binney and others (1985) has discovered exposures in the north where the Meguma rocks are overturned dipping at high angles to the north.

The boundary between the Halifax and Goldenville Formations has been offset by steeply dipping faults in Domain I. Binney has found two sets of strike slip faults. One set consists of faults trending about 340 degrees with offsets measured from 10 to 150 m. The second set of faults trend from 010 to 030 degrees, and offset the boundary by 200 to 500 m.

2.3.2c Petrography

The two main rock types of the Meguma Group, quartz metawacke and slate, have behaved differently under the regional metamorphic conditions of the Acadian Orogeny. This difference in response can be attributed to the original variation in composition of the Meguma sediments. The quartz metawacke generally consists of porphyroblasts of quartz and xenoblastic spessartine garnets in a matrix of more elongate quartz grains, muscovite, and lesser amounts of chlorite and plagioclase. The contorted quartz metawacke of Lithology 3 is unique. In this case the quartz metawacke has a high modal percentage (up to 80%) of small, xenoblastic spessartine garnet porphyroblasts contained in a groundmass of muscovite, quartz, rutile, chlorite, and oxide

needles. This unit may also have carbonate in the matrix accounting for its calcareous nature. These metawackes also tended to have compositional banding, alternating layers of mica rich (chlorite and/or muscovite) zones, and more quartz rich zones. The carbonate is distributed throughout both of these compositional bands. The presence of sphalerite and galena in the calcareous quartz metawacke is fracture controlled. Pyrrhotite and pyrite are more common, and occur as separate beds or individual blebs in the quartz metawacke.

The black slates typically consist of small porphyroblasts of quartz, chlorite, and spessartine garnet in a groundmass composed of abundant graphitic material, quartz, muscovite, and opaque needles. Two classes of garnet porphyroblasts have been observed in the slates. One class is large (3 mm), idioblastic garnets with radial carbonaceous inclusions, and more rare muscovite inclusions. The second class of spessartine garnets are smaller, more xenoblastic, often with cores of pyrrhotite or pyrite. Pressure shadows of predominantly quartz and small amounts of muscovite exist in association with individual spessartine garnet grains and unique agglomerates of smaller garnets surrounding an iron sulphide core. Blebs of pyrite and pyrrhotite have pressure shadows of undulose, elongate quartz. The texture indicates that the iron sulphide mineralization and spessartine garnet predate the formation of the slaty cleavage (Jenner, 1982).

The most significant observation made in the petrographic study of the regional metamorphic rocks was the discovery of sphalerite in the core of spessartine garnets in the black slates. The sphalerite is orange to red under transmitted light, and an intermediate grey when viewed in reflected light. The presence of sphalerite in the core of the regional metamorphic spessartine garnets indicates that the zinc mineralization occurred prior to the regional metamorphic event. This results in an age greater than 400-415 million years for the zinc mineralization. Intrusion of the granitoid pluton and associated contact metamorphism followed regional metamorphism, and are therefore younger than the mineralization. This fact suggests that the heat of the intrusion potentially could influence the distribution and style of mineralization.

Where interbedded with quartz metawacke, the slates often contain greater concentrations of the sulphide minerals. In the black slates, sphalerite and galena are present mainly in fractures, and infrequently occur as blebs. The pyrite and pyrrhotite formed in beds, and are also found as rounded and elongate blebs.

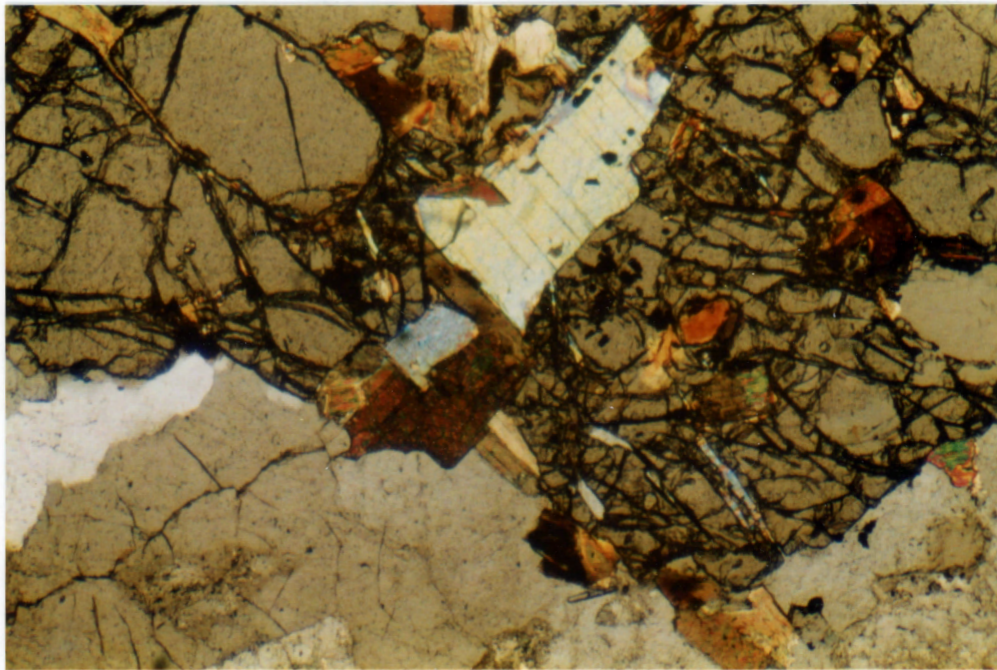
2.3.3 Domain II - Granitoid Pluton

The regionally metamorphosed rocks of Domain I were intruded by a granitoid pluton in the southeastern section of the study area. The intrusion is a granodiorite-monzogranite complex similar to other granitoid

bodies in southern Nova Scotia. Aplite dykes were not found in the study area, although this may be attributed to limited outcrops. A pegmatite phase was exposed in the north, however field relations could not be determined to indicate whether its occurrence was as a dyke or as the cupola of the pluton.

Biotite granodiorite was located close to the contact of the granitoid with the Meguma rocks in Cox Brook. The granodiorite is grey-dark grey, medium grained and somewhat equigranular. Microscopically, the alkali feldspar forms the largest grains in a groundmass of biotite, plagioclase, quartz, small alkali feldspar, secondary chlorite, and accessory garnet and zircon (Figure 2.5). Biotite is a major constituent with a modal abundance close to 20%. No xenoliths were found in the granodiorite phase of the studied pluton. Further field work is necessary to search for enclaves in this phase of the pluton.

The monzogranite forms a large volume of the granitoid pluton at Eastville. This phase of the pluton consists of texturally distinct phases defined on the basis of grain size and alkali feldspar phenocryst content. The monzogranite ranges from medium grained to a micropegmatite. Variations in the alkali feldspar phenocryst content is responsible for a range in colour of the rocks. The monzogranite is a grey colour closer to the granodiorite, and very leucocratic (white) further to the southeast. Petrographic studies showed the mineralogy of the



— .5 mm —

Figure 2.5 Garnet in the granodiorite with inclusions of biotite and muscovite.

monzogranite is different from the granodiorite. Alkali feldspar is more abundant, and usually forms phenocrysts in a groundmass of quartz, plagioclase, muscovite, biotite, smaller alkali feldspar and accessory zircon. The monzogranite may be distinguished from the granodiorite phase on the basis of less biotite and increased muscovite content.

A metasedimentary enclave was found in the monzogranite phase of the granitoid pluton. The enclave was rounded with a hornfelsic texture. The grain size is fine to medium, which represents an increase in grain size from the average regionally metamorphosed Meguma rock. The enclave has a granoblastic texture, and consists of quartz, sericite, biotite, alkali feldspar, and embayed garnets. Sericite is very abundant, and likely has resulted from replacing plagioclase. It can be concluded the enclave represents a xenolith due to its mineralogy and appearance being identical to a quartz metawacke of the Goldenville Formation.

There are various indications of deformation in the granitoid rocks at Eastville. Alignment of micas (biotite and muscovite) was observed in a number of the granitoid thin sections. During the field studies foliations were identifiable only in a few of the specimens. Quartz in the granodiorite and monzogranite often has undulose extinction indicating deformation. Also the pegmatite at Eastville is

mylonitic in that it is highly foliated with localized zones of intense deformation defined by lineated, fine grained minerals. Megacrystic alkali feldspar is sometimes preserved in these narrow zones. Mylonites form by ductile deformation associated with shear zones and faulting. Kinking in the cleavages of the micas has been observed indicating shear forces on the pluton. The deformation may be related to the St. Mary's Fault, located just 25 km east of Eastville, or to the numerous faults to the immediate west.

2.3.4 Domain III - Contact Metamorphic Zone

2.3.4a Stratigraphy

Whereas the regional metamorphic rocks of Domain I consisted of a complete stratigraphic section, Domain III does not show a conformable relationship between the Goldenville and Halifax Formations. This can be related to the low angle thrust fault in the northeast of the study area. Lithology 1 is still present as a massive, impure quartz metawacke. The Transition Zone of Lithology 2 varies in thickness due to faulting in the vicinity of the thrust. Lithology 2, consisting of both quartz metawacke and slate, includes a brecciated quartz metawacke in a purplish coloured matrix. The contorted, manganiferous beds of Lithology 3 are absent in Domain III either due to the complex faulting or the influence of the granitoid pluton.

An absence of carbonate in Domain III can be attributed to the removal of the contorted beds from the stratigraphic section. The contact of the Goldenville and Halifax Formations has been determined by the presence of the fault zone in this domain. Lithology 4 is composed of the Halifax Formation, and consists of slate blocks and quartz metawacke. Due to the close proximity of the granitoid (within 700 m), the deeper drill holes have encountered schists, which may be more foliated equivalents of either quartz metawacke or slate.

2.3.4b Structure

The beds of the Halifax and Goldenville Formations are slightly more steeply dipping in Domain III. The contact metamorphism and distinct cleavage has obliterated the bedding in most cases making it difficult to determine the attitude. Glacial overburden is thickest in this area contributing to the problem of bedding measurements. Three cleavage directions have been observed in the slates in the contact zone of the granitoid pluton.

A low angle thrust fault is the most obvious structural element in the eastern section. A topographic break allows the trace of the fault to be followed in the field. The thrust fault is offset in its western extent by a strike slip fault trending 350 degrees (Binney et al., 1985).

Core logging has revealed a structural history that is possibly more complex. A sequence of fault sheets may exist

in the area of the thrust fault displacing units from their original positions in the section. This is suggested by the occurrence of fault gouge at various stratigraphic levels. Binney has suggested the fault predated the intrusion of the granite based on the continuation of the metamorphic aureole from one side of the thrust fault to the other. Sheared andalusites, often replaced by sericite, have been observed in the fault zone. This contradicts Binney's interpretation and suggests the fault movement was after the emplacement of the granitoid. The presence of any contact metamorphic mineral in the fault gouge would support this interpretation.

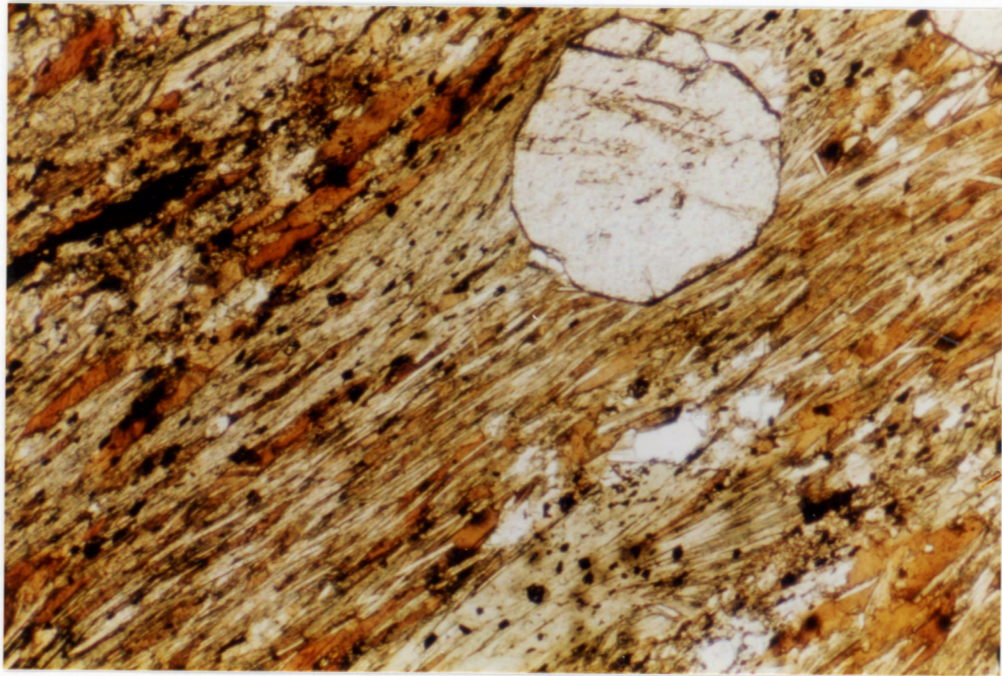
2.3.4c Petrography

The contact metamorphic rocks of Domain III show an increase in the degree of metamorphic recrystallization as the contact with the granitoid intrusion is approached. This relationship implies that the heat associated with the intrusion was the most important agent responsible for the reconstitution of the fabric and composition in these rocks. Biotite is considered to be a contact metamorphic mineral as it occurs solely in the more eastern drill holes, and is absent in all lithologies in the west. Biotite was absent in rocks at depths over 200 m in the west, but was present as small grains in the quartz metawacke at depths between 75 and 100 m in the central drill holes. The dipping contact of the granitoid was shallow enough to begin affecting the

lower sections of holes drilled in the central region of the study area.

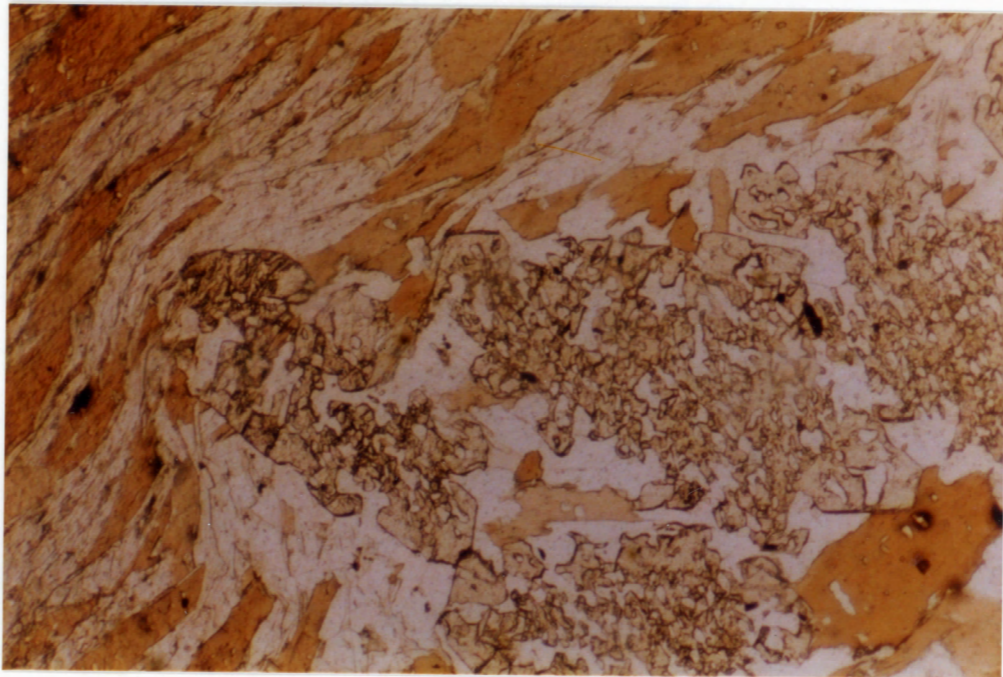
Five types of areas can be created on the basis of the dominant mineral assemblages. These are (1) a biotite zone characterized by biotite with spessartine garnet; (2) an andalusite zone characterized by two varieties of andalusite and biotite, localized to graphitic layers of the Halifax slates; (3) a garnet zone characterized by almandine garnet, andalusite, and biotite; (4) a garnet zone similar to type 3 except andalusite is absent; and (5) a staurolite zone characterized by staurolite, almandine garnet, and biotite. Figures 2.6 and 2.7 show examples of two of these assemblages.

In all of the contact metamorphic rocks surrounding Hattie Lake Pluton biotite and muscovite are the dominant matrix minerals, defining a schistosity by their subparallel arrangement. With increasing grades of metamorphism, especially in the quartz metawacke, biotite tends to become more porphyroblastic and more randomly oriented. The biotites change from smaller flakes in lower grades to larger, equidimensional, xenoblastic grains in higher grades. Chlorite, elongate quartz, and oxide needles define the foliation less commonly than biotite and muscovite. Often in the higher grades, bands of alternating mica-rich and quartz-rich layers develop. Occasionally chlorite will occur as porphyroblasts parallel to the fine oriented grains defining the foliation. Chlorite increases in abundance



.5 mm

Figure 2.6 Garnet biotite schist from the contact aureole.
The almandine garnet overprints the foliation defined
by biotite and muscovite.



.3 mm

Figure 2.7 Staurolite-garnet-biotite schist representing the
the highest grade of metamorphism reached.

when it occurs as a retrograde mineral. It may appear in large agglomerates associated with breakdown of garnet and biotite.

Andalusite occurs only in the eastern section of the deposit, and therefore is considered a contact metamorphic mineral. The andalusite appears as large porphyroblasts (5 mm) in two forms, as regular andalusite and its chiastolite variety. The chiastolite is restricted to the graphitic layers of the Halifax slates, probably due to the high original Al content of these sediments. The characteristic carbonaceous cross is very evident, and abundant oxide needle inclusions form in the chiastolite. The inclusions occur in two orientations, neither parallel to the foliation. One orientation runs diagonally parallel to one cross, and the other is parallel to one face of the andalusite prism. Andalusite is sheared in some of the drill core samples, appearing very elongate and sometimes completely retrograded to sericite. Its optical properties included high relief, two cleavages, and a biaxial negative figure with a $2V=65$ degrees. The regular variety is often more elongate in one direction, whereas the chiastolite had a square cross section.

Garnet occurs in two forms in the contact zone of the pluton. Spessartine garnet occurs as small, subidioblastic to xenoblastic grains about .2 mm in diameter. These garnets occur in clusters, but seem rather unstable under the conditions of contact metamorphism. Spessartine garnets

usually form at lower temperatures and pressures than almandine garnets (Winkler,1974). Corroded and embayed grain boundaries in the lower grades suggest they will be unstable at the higher grades. Almandine garnets occur at higher grades, and are very distinct from the spessartine variety. They are a light red-brown, subidioblastic to idioblastic, and large up to 5-6 mm. These garnets overprint the matrix minerals defining the foliation in the contact zone. This indicates the contact metamorphic garnets formed after the development of the schistosity. The almandine garnets may have relatively few inclusions or in some instances they can be abundant. Quartz and oxide needles (ilmenite) are the most predominant inclusions. The inclusions are roughly aligned to the foliation suggesting syn- to post-tectonic growth of the porphyroblasts. The garnets are often fractured, and commonly have retrograde chlorite associated. Almandine garnet tends to be most abundant and largest in biotite-rich contact metamorphic rocks. In the very quartz-rich metawackes the garnets are small and xenoblastic.

Staurolite is present as very distinct grains in the highest grade rocks. The staurolite forms large (up to 6 mm), idioblastic grains with a sieve texture. The circular inclusions consist of predominantly quartz, biotite, and infrequently garnet. The staurolite is a light yellow in plane polarized light, and has a characteristic diamond cross section. The staurolite overprints all metamorphic

constituents, apparently including everything as it grows.

The presence of chlorite and sericite replacing garnet and andalusite respectively, indicates a retrogressive event. Pseudomorphs retain the euhedral outline of the host mineral, and occasionally remnants of the original mineral can be found in the core. Pseudomorphic textures are consistent with a static thermal event accompanied with little deformation (Novak and Holdaway, 1981).

The contact metamorphosed rocks are apparently less mineralized than the regional metamorphic rocks discussed earlier. The schists occurring near the granitoid are unmineralized. The mineralization that is present is concentrated around the low angle thrust fault. Pyrite and pyrrhotite are ubiquitous in the less foliated sections of the Halifax slates. Sphalerite and galena are found in the blocks at the base of the Halifax Formation. The economic ore minerals are also found present in the fault gouge associated with the thrusting in the eastern section.

2.4 Glacial Deposits

Glacial till covers much of the low lying area around Eastville. In the western section of the deposit Cox Brook forms a deeply incised valley which reveals till thicknesses up to 10 m. In the eastern part large granitic boulders are abundant indicating the close proximity of the granitoid pluton. A program of basal till sampling was carried out by

St. Joseph Explorations Limited to assess the extent of the Eastville deposit (Binney,1981).

Most of the holes were drilled 2-3 m deep with a 4-inch auger. Holes up to 6 m deep were possible, and often over drumlins this depth was drilled. Samples that were obtained from the drilling were analyzed for Pb, Zn, Fe, Mn, As, Ba, Sb, and Sr. The results of St. Joseph Explorations' till analyses showed that the metalliferous area is larger and more intense to the west. Pb and Zn increases to the west along with Ba, Mn, As, and Fe. In the eastern section of the deposit, Pb and Zn was also found to be high around a low angle thrust fault, indicating metal concentration may occur along the line of this fault. Ba and Mn anomalies were confined to areas where the calcareous metawacke formed the bedrock. Sr increases to the east where the other elements decreased. This may be a result of the granitoid pluton.

2.5 Summation

A study of the local geology around Eastville has shown two rock groups to predominate. The Meguma Group dominates in the west, and is intruded in the east by a granitoid pluton. Closer examination of the granitoid rock revealed two zones consisting of a granodiorite and monzogranite phase of the pluton. In the far west, the Meguma Group formed a complete stratigraphic section with a conformable boundary between the Goldenville and Halifax Formations. As

the pluton is approached to the east the conformable contact relationships between the two formations is lost. A fault zone marks the contact between the Goldenville and Halifax Formations within 600 m of the pluton. Full understanding of the rocks of the Eastville deposit is impossible without consideration of their geochemistry.

Chapter 3 Trace Element Geochemistry

3.1 Igneous Rocks

The trace element chemistry of nine samples taken throughout Hattie Lake Pluton is presented. The powdered samples were analyzed by x-ray fluorescence for fifteen trace elements (Ba, Rb, Sr, Y, Zr, Nb, Th, Pb, Ga, Zn, Cu, Ni, TiO₂, V, and Cr). Of the nine samples collected, visual studies in the field classified three as granodiorite, and the other six as monzogranite. One of the six monzogranites was a pegmatite consisting of large alkali feldspar phenocrysts. This study of the trace element data compares the chemical character of Hattie Lake Pluton to the South Mountain Batholith of Nova Scotia.

3.1.1 Trace Element Study of the Granitoid

Trace element studies have been very useful in the understanding of granitoid rocks. The trace element data for the nine granitoid samples are presented in Appendix 1. The granodiorite and monzogranite of Hattie Lake Pluton show obvious differences in their trace element contents. Table 3.1 shows the average trace element contents of the granodiorite and monzogranite phases. The table includes for comparative purposes data on the South Mountain Batholith collected by McKenzie and Clarke(1975).

The basic chemical character of the granodiorite implied by the mineralogy in petrographic observations is confirmed

by the trace element data. The granodiorite is enriched in Ba, Sr, Y, Zr, Nb, Zn, Th, Cu, TiO₂, V, and Cr. Relative to the monzogranite only Rb is depleted in the granodiorite phase. Pb, Ga, and Ni remain relatively unchanged in the granodiorite and monzogranite phases of the pluton. These elements which are enriched in the granodiorite should vary antipathetically with increasing differentiation (Taylor, 1965). These data imply the granodiorite is a less differentiated phase of the pluton. This point can be investigated further by evaluating possible differentiation trends.

Table 3.1 Average Trace Element Content of the Granodiorite

Trace Elem.	Granodiorite		SMB Monzogranite		SMB	
	Mean (ppm)	St.Dev.	Mean (ppm)	Mean (ppm)	St.Dev.	Mean (ppm)
Ba	883.67	73.1	667.3	366.00	163.0	253.9
Rb	145.00	5.29	147.3	204.33	25.8	334.0
Sr	231.00	15.7	138.4	69.67	41.9	28.0
Y	26.67	4.93	--	9.17	3.97	--
Zr	251.33	16.9	206.3	73.67	44.9	85.2
Nb	15.00	1.00	--	9.33	1.37	--
Th	10.67	2.52	--	6.00	3.90	--
Pb	26.67	9.61	--	25.67	4.89	--
Ga	21.67	1.53	--	20.50	2.17	--
Zn	97.33	15.9	67.8	47.83	17.2	60.0
Cu	4.00	2.00	--	-4.50	1.87	--
Ni	8.67	1.15	--	5.33	1.51	--
TiO ₂ (wt.%)	.903	.055	.61	.205	.160	.24
V	64.33	11.7	--	9.00	12.1	--
Cr	24.33	2.08	--	10.00	9.14	--

The plot of Ba vs Rb shows a normal differentiation trend as shown in Figure 3.1. Ba is enriched in the granodiorite, while Rb, which behaves similarly to K, is concentrated in the late crystallizing phase of the

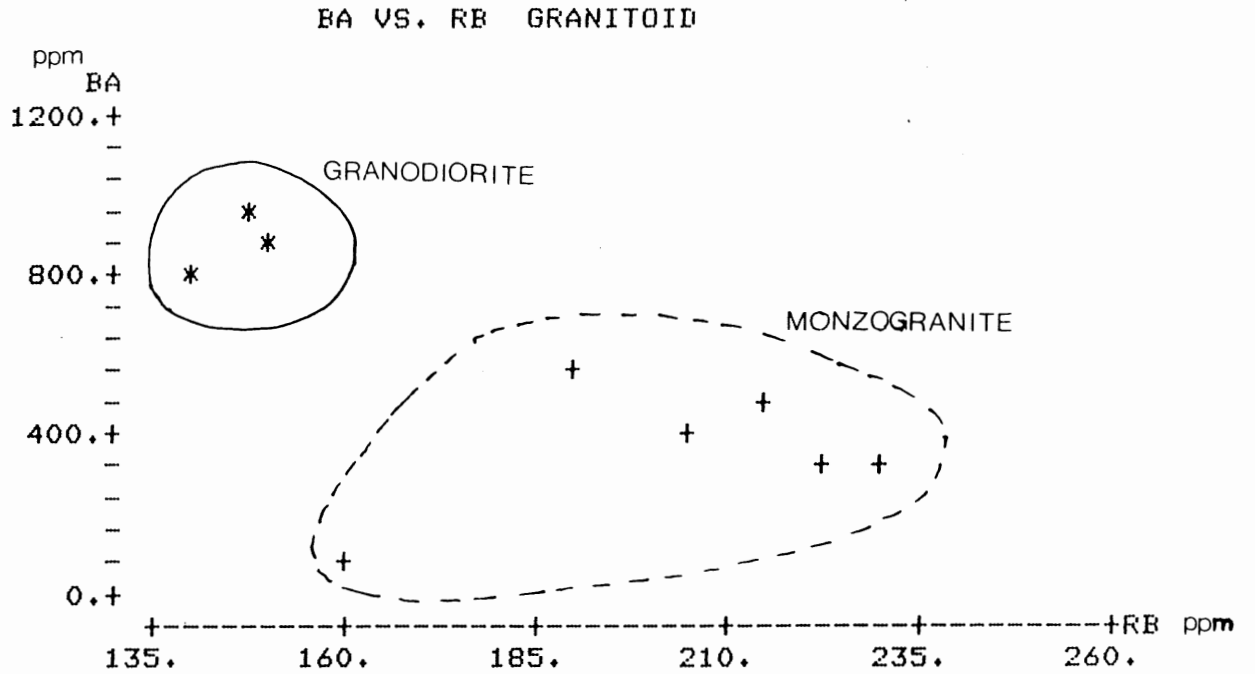


FIGURE 3.1 Differentiation trend of Ba enrichment and Rb depletion in the granodiorite phase.

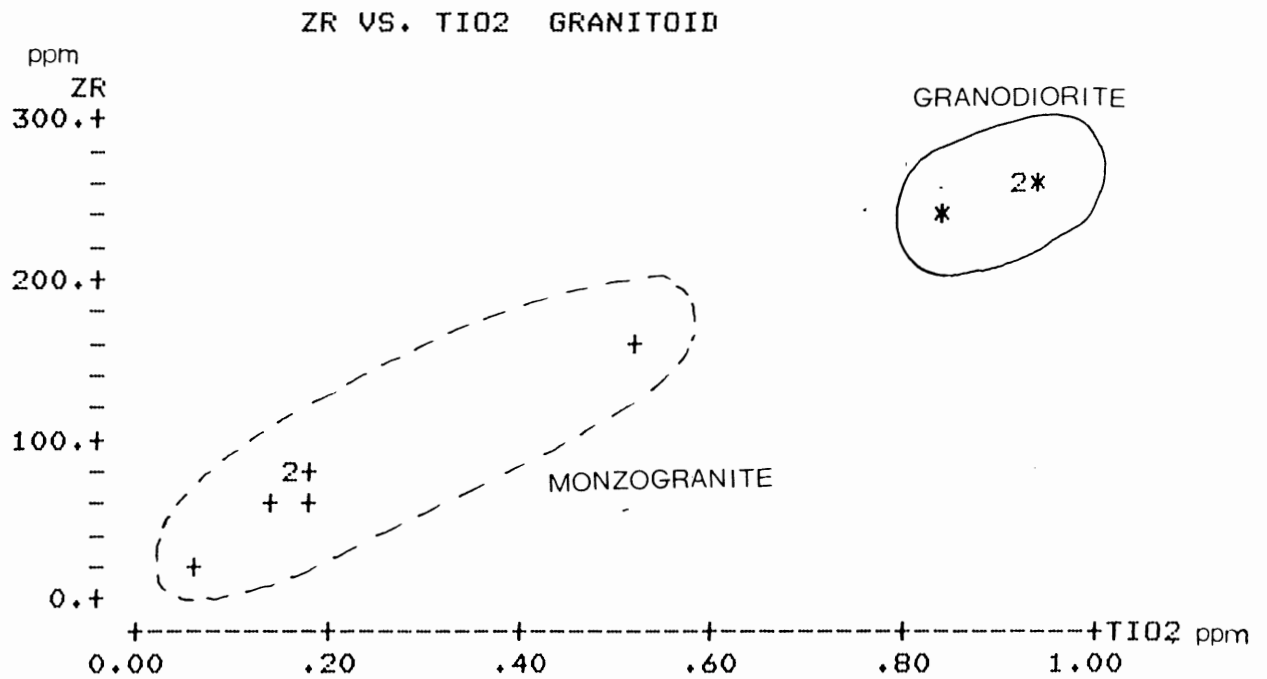


FIGURE 3.2 DIFFERENTIATION TRENDS - Both Zr and Ti are enriched in the granodiorite.

monzogranite, where alkali feldspar is modally important. Ba enters the early formed K minerals, and is not depleted in the magma until very late in the differentiation sequence (Taylor, 1965).

Zr and TiO_2 are plotted in Figure 3.2, and show a very different relationship from Ba-Rb. The linear relationship shows a uniform depletion of Zr with TiO_2 , which also decreases with differentiation. Ti enters into the biotite of the crystallizing granodiorite, while Zr goes mainly into zircon, which also forms early in the crystallization sequence.

Ternary plots were constructed to further illustrate the distribution of trace elements in the two main phases of the pluton. The plot of Rb-Sr-Ba given in Figure 3.3 shows the trend of differentiation between the two well separated groups of points representing granodiorite and monzogranite. The granodiorites show an enrichment in Ba, and a slight concentration of Sr, while Rb is strongly concentrated in the monzogranite. Rb is taken up in the late formed alkali feldspar, and Sr enters plagioclase feldspars, which along with biotite is abundant in the granodiorite.

Triangular plots of Rb-Ba-Zr and Rb-Sr-Zr both show excellent trends of differentiation. The plots are presented in Figures 3.4 and 3.5. Both plots show a strong trend toward Rb with increased differentiation. The granodiorites show enrichment in Ba-Zr and Sr-Zr, plotting distinctly separate from the monzogranite field.

RB-SR-BA GRANITOID

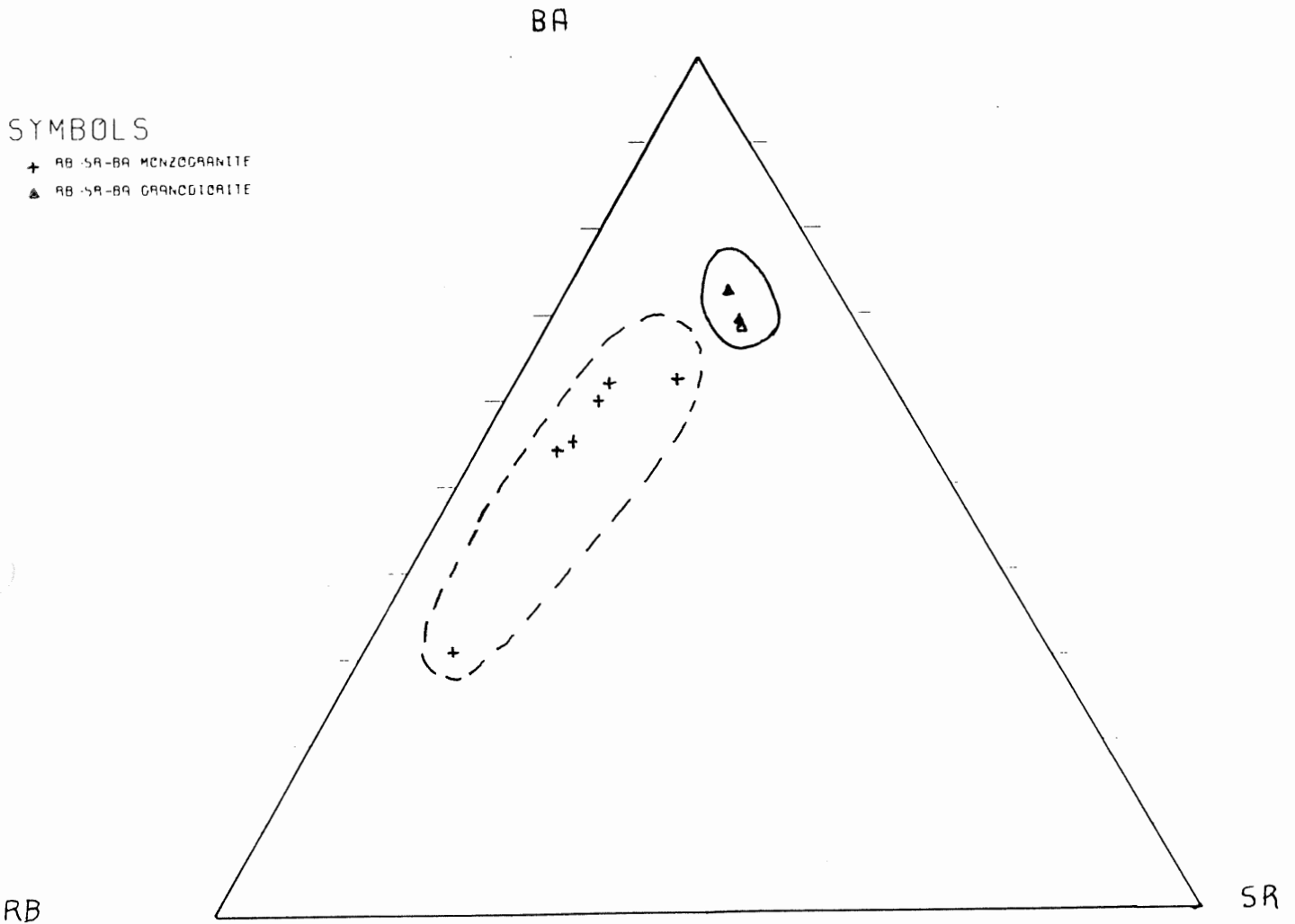


FIGURE 3.3 Triangular diagram showing trends toward Ba and Sr enrichment with increasing differentiation.

RB-BA-ZR GRANITOID

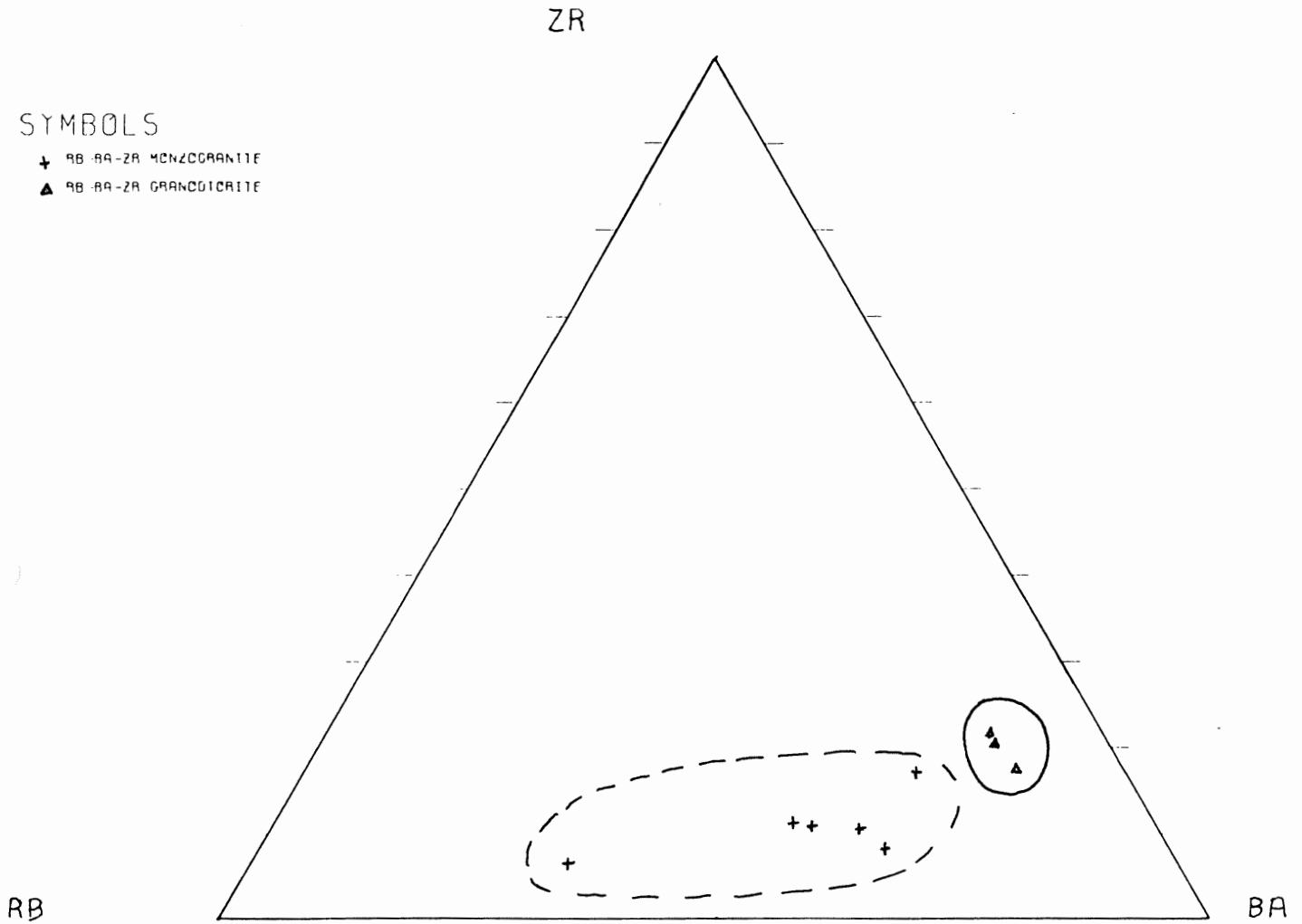


FIGURE 3.4 Triangular diagram showing trend toward Ba and Zr enrichment with increasing differentiation.

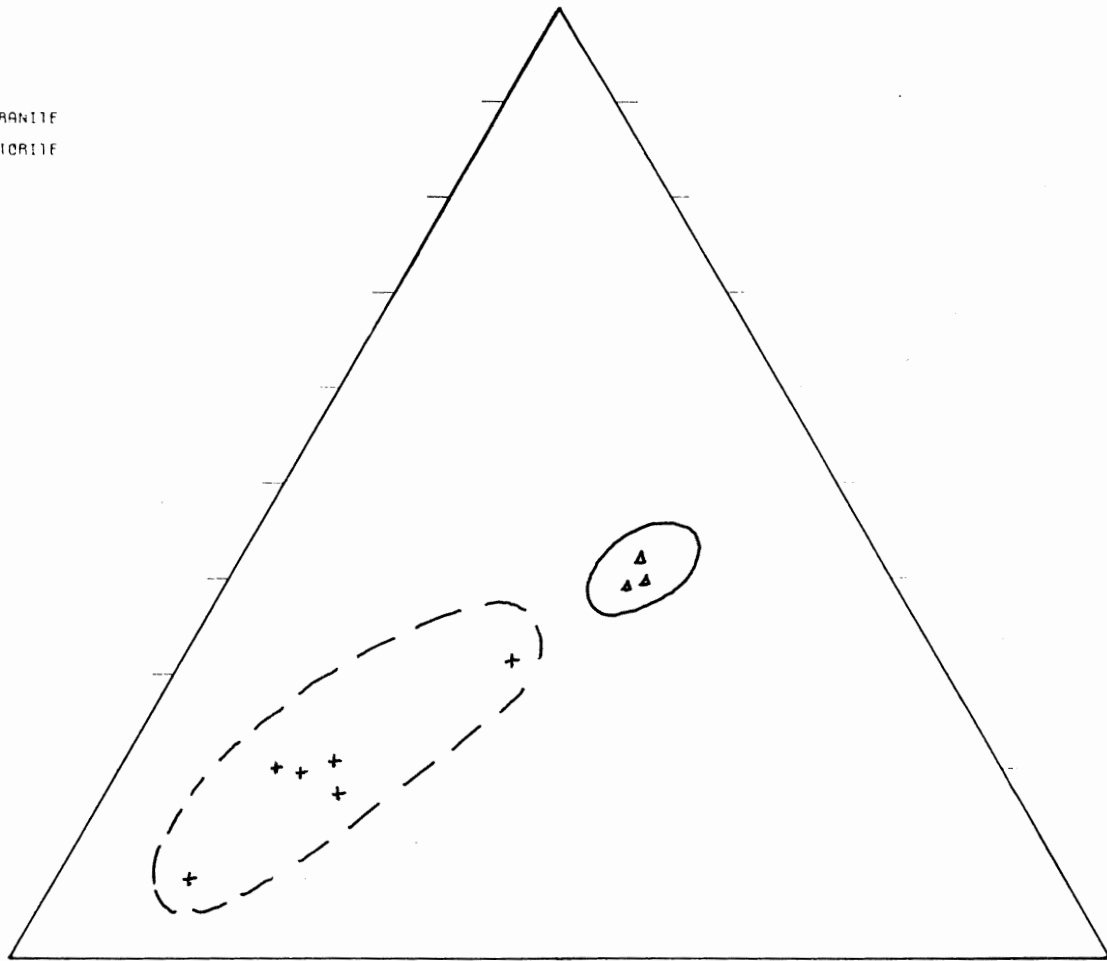
RB - SR - ZR GRANITOID

ZR

SYMBOLS

- + RB - SR - ZR MONZOGRAHITE
- ▲ RB - SR - ZR GRANODIORITE

RB



SR

FIGURE 3.5 Triangular diagram showing trend toward Sr and Zr enrichment with increasing differentiation.

PB-ZN-CU GRANITOID

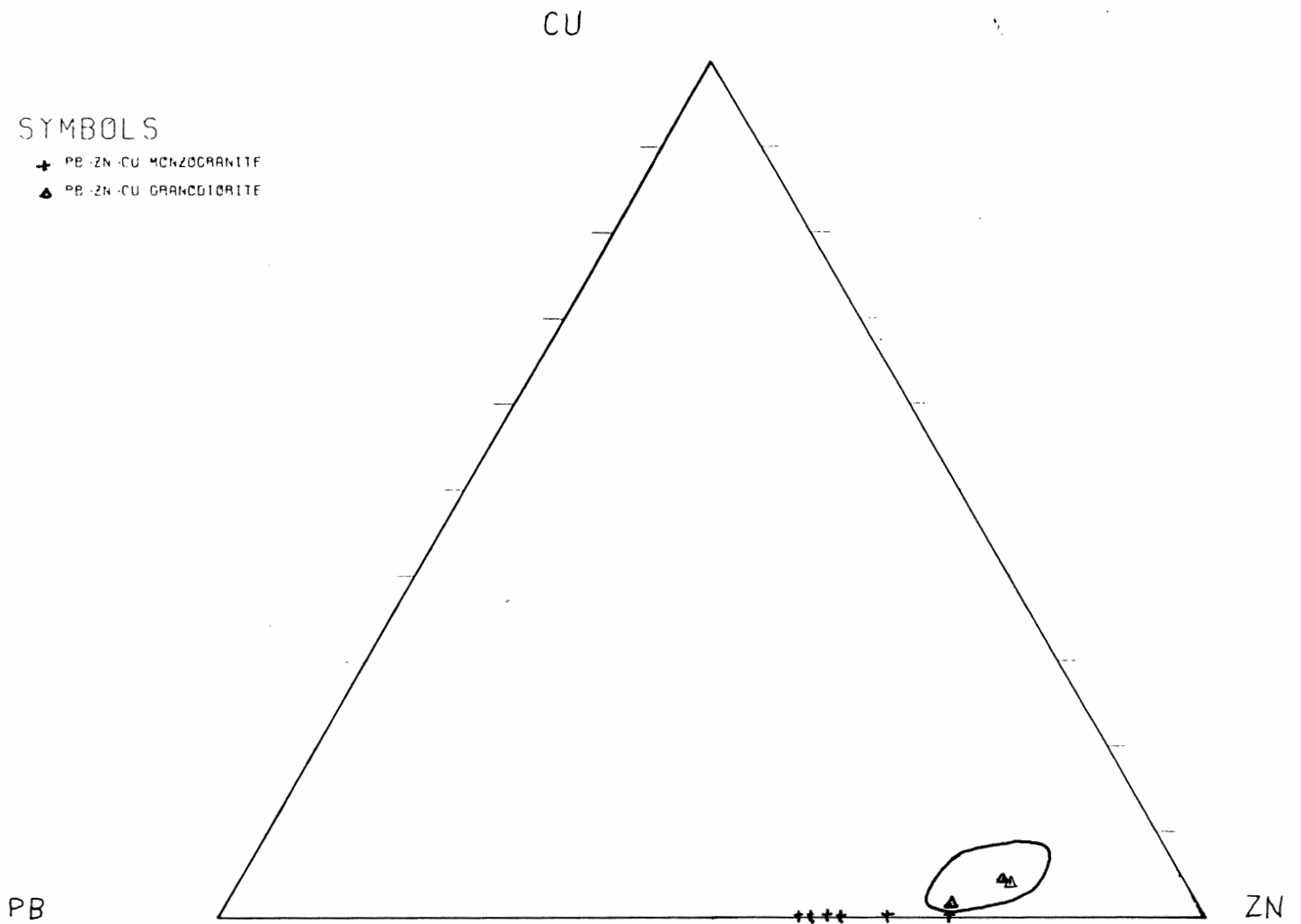


FIGURE 3.6 Triangular diagram showing that Cu is concentrated in the granodiorite. Note the Pb:Zn ratio is close to 1:2.

Figure 3.6 is ternary plot of Pb-Zn-Cu. The two groups of data points highlight another difference between the chemical characteristics of the granodiorites and monzogranites. Zn and Cu show enrichment in the granodiorites relative to Pb. Zn is partitioned into biotite, and because biotite is modally more abundant in the granodiorite, the isolation of the granodiorite field is not unexpected. Cu may also be concentrated in the biotite or it may also enter into early forming plagioclase. Pb can be expected to occur in both alkali feldspar and mica, and thus shows no preference for late or early stage magmas. Chatterjee and Strong (1984) found Cu to be enriched in greisens in the western section of the South Mountain Batholith. Cu is totally absent from the late crystallizing phase of Hattie Lake Pluton, and is only a very minor component of the granodiorites.

3.2 Meguma Group

The trace element chemistry of 25 samples spanning the entire length of Drill Hole 26 in the eastern section of the Eastville deposit is presented. The samples were analyzed by x-ray fluorescence for the same trace elements as the granitoid rocks in the previous section. The trace element data will be studied to gain some information on the possible character of the parent rock, and to investigate the distribution of the base metals in the eastern section of the deposit.

3.2.1 Trace Element Study of Drill Hole 26

The trace element data for Meguma rocks of Drill Hole 26 are presented in Appendix 2.

Identification of the parent rock from which the Meguma sediments were derived will be attempted by comparing the trace element composition of the metamorphic rocks to the average trace element content of known rocks. A ternary plot of Rb-Sr-Ba for the Meguma Group of Hole 26 contains a large grouping near the Ba apex. The plot is shown in Figure 3.7. There is a slight trend towards Sr, but Rb seems to vary little. This group of plotted points falls close to the granodiorite field of the comparable igneous plot. A second plot of Rb-Sr-Zr was done to confirm this relationship, and the results are shown in Figure 3.8. The points again fall in a large cluster, this time a bit to the right of centre of the triangular diagram. Comparison with the equivalent igneous plot of the previous section shows that this field is close to the granodiorite composition. Assuming little mobilization of elements due to weathering, it seems the Meguma sediments were derived from a granodiorite parent rock.

A plot of Pb-Zn-Cu was performed to show the variation of base metals in the drill hole. The plot is shown in Figure 3.9. There is a small trend toward Cu and a small variation in the Pb:Zn ratio, but for the most part the plot forms one cluster. The data clusters about a Pb:Zn ratio

RB - SR - BA HOLE 26

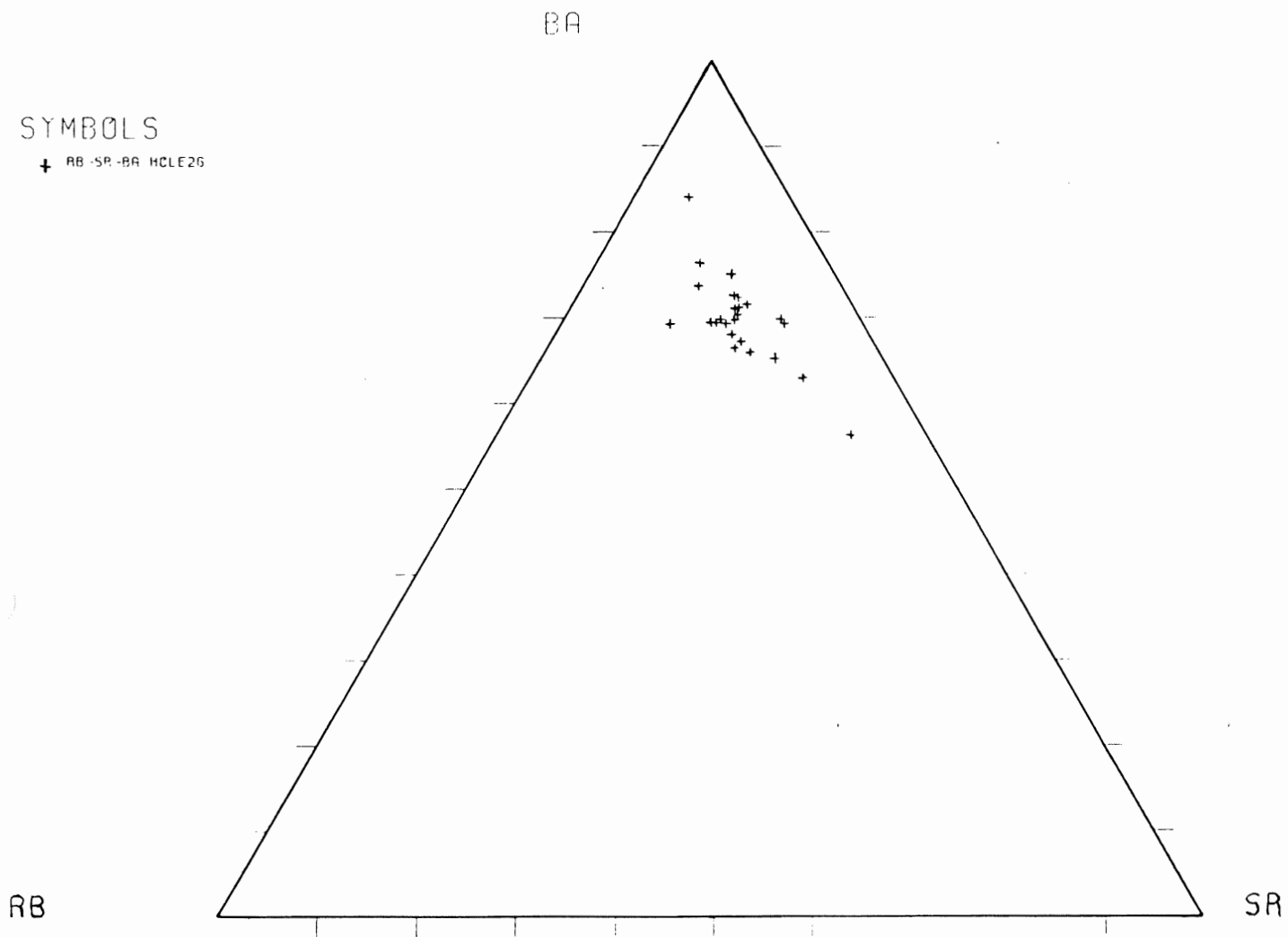


FIGURE 3.7 Triangular diagram for the Meguma rocks showing a cluster of points near the Ba apex.

RB - SR - ZR HOLE 26

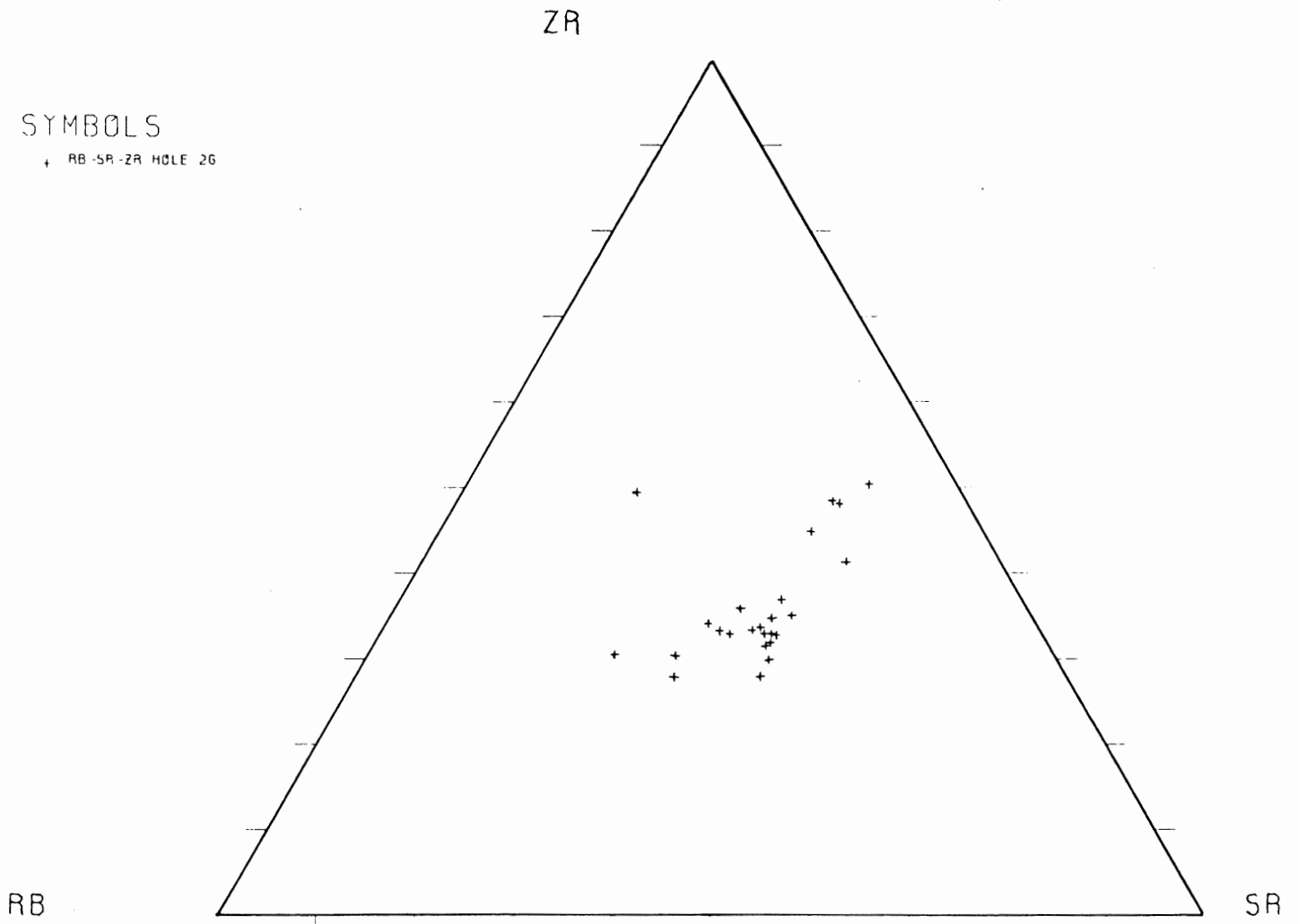


FIGURE 3.8 Triangular diagram for the Meguma rocks showing clusters very similar to those of granodiorite rocks (Figure 3.5).

PB-ZN-CU HOLE 26

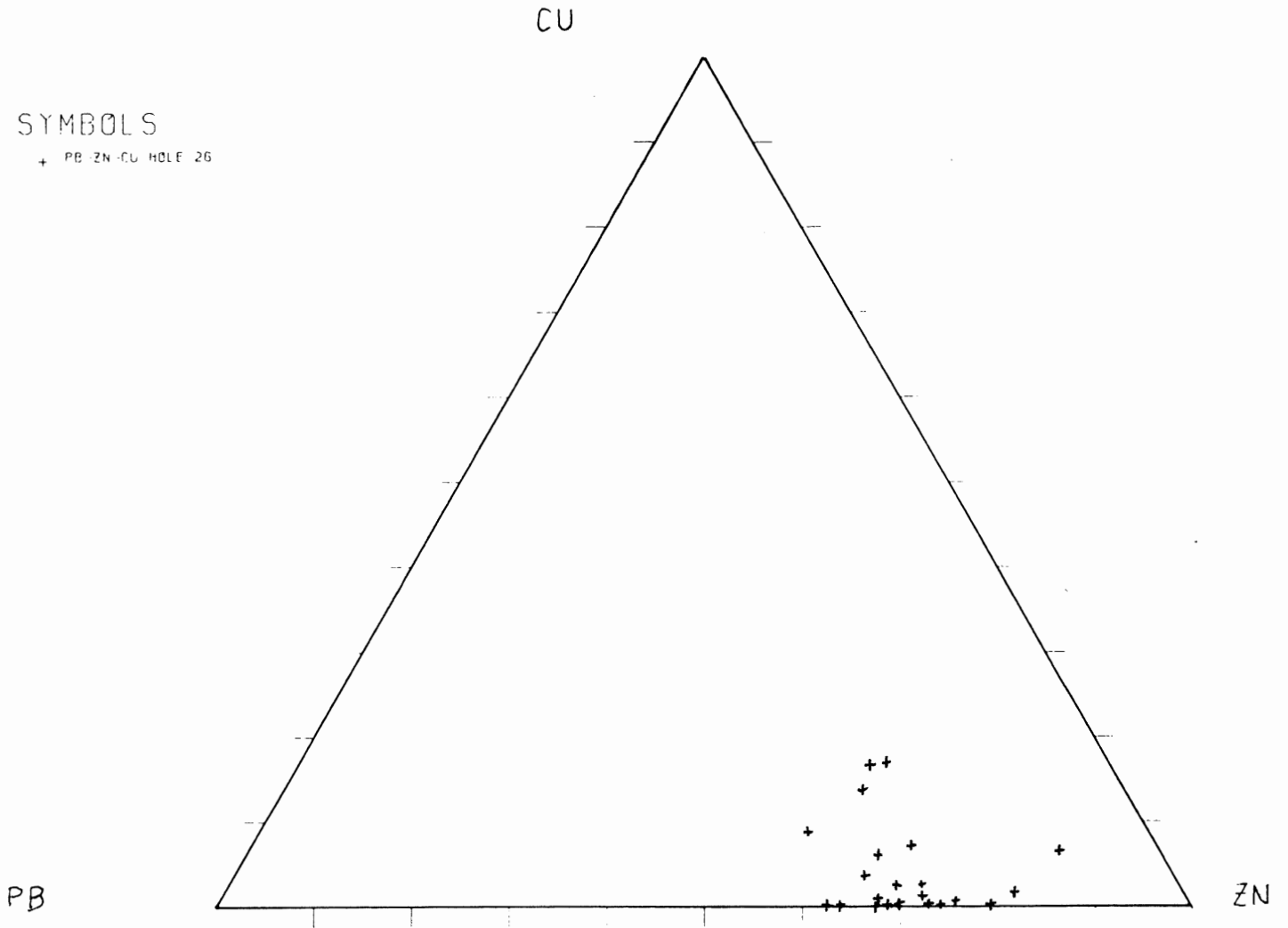


FIGURE 3.9 Triangular diagram of base metals in the Meguma Group showing a Pb:Zn ratio of around 1:2.2.

close to the 1:2.2 found by Binney et al. (1985) for drill holes in the western section of the deposit. The fact that all points plot in the same general area away from Cu indicates that the lithologies comprising the section were mineralized to the same degree. Pb and Zn in the metasedimentary rocks are greatly in excess of Cu. Also of interest is the fact that the Pb:Zn ratio in Hole 26 is very close to the ratio found in the granites of this study.

3.3 Summation

The chemical data have supported field classifications of the granitoid samples. The trace element data illustrate a comagmatic, differentiated suite of granitic rocks similar to the South Mountain Batholith. Graphical plots revealed differentiation trends that can be explained by the predicted distributions of the trace elements in the minerals forming either phase. It is speculated that the Meguma Group of Hole 26 may have been derived from a parent rock of similar composition to a granodiorite. Liew (1982) came to a similar conclusion about a section of the Goldenville Formation he studied at Taylor's Head, Nova Scotia. The Pb:Zn ratio in Hole 26 compares closely to that of drill holes from the western section of the deposit. It is often true that the whole rock geochemistry is influenced by the mineralogy of the rocks.

Chapter 4 : Mineral Analyses

4.1 General Statement

The chemical compositions of garnet, biotite, chlorite, muscovite, staurolite, andalusite, ilmenite, rutile, and plagioclase were determined by microprobe analysis. The results are shown in Tables 4.1 to 4.8. Mineral analysis was undertaken for a number of reasons. Generally it was hoped the investigation would provide additional information on the chemical effects of the contact metamorphism at Eastville. An examination of the data for certain minerals might yield trends in specific elemental ratios. More specifically, the pattern of garnet zoning in the Meguma metasedimentary rocks can be compared to that exhibited by the garnets in the granitoid. The mineral compositions might allow the use of garnet-biotite geothermometry based on Fe-Mg partitioning. The results of the microprobe analyses for each mineral are discussed in the above context.

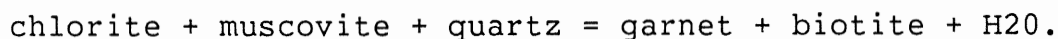
4.2.1 Garnet

4.2.1a Garnets of the Meguma Group

The metasedimentary rocks of the Meguma Group contain two varieties of garnet. The regionally metamorphosed rocks contain small spessartine garnets, while almandine garnets exist in the higher grade rocks of the contact aureole.

Most of these garnets probed show 'normal' zoning with increasing Fe and Mg, and decreasing Mn and Ca from the core to the rim.

The garnets show a marked increase in Mg/(Mg + Fe) from .096 to .120 with increasing metamorphic grade. This can be interpreted to define a continuous reaction by which garnet forms at the expense of chlorite (Sivaprakash,1981) :



The observed normal zoning of Mn decreasing and Mg/(Mg + Fe) increasing from core to rim in ZGB-0164 agrees with the formation of garnet by this reaction (Table 4.1a). The almandine garnet has a very low Mg/(Mg+Fe) ratio that ranges from .089 to .128. Low Mg/(Mg+Fe) ratios favour the formation of staurolite over cordierite at higher grades.

Table 4.1a Chemical Trends in Metamorphic Garnets

	ZGB-0164 (Garnet Zone)	ZGB-0216 (Staurolite Zone)
Mg/(Mg+Fe)	0.096	0.120
MnO (wt.%) -rim	8.85	4.25
MnO (wt.%) -core	10.90	4.80
Mg/(Mg+Fe)		
core	0.089	
rim	0.095	

Table 4.1b gives the compositions of five garnets occurring in the Meguma Group. The samples have been arranged in a sequence from lowest to highest grade.

4.2.1b Garnets in the Granitoid

Microprobe analysis was performed on two grains of garnet from a specimen of granodiorite taken close to the contact with the Meguma rocks (Table 4.1c). A detailed traverse was taken across the diameter of a large garnet (2 mm) to examine the zoning pattern, and determine whether the garnets are magmatic or metamorphic in origin. The results of the traverse are shown in Table 4.1d. The rim and core compositions of the smaller garnets confirmed the observed profile. The granitoid garnets are light brown, subidioblastic with inclusions of biotite, muscovite, and oxide needles. No reaction rims were observed to surround the fresh grains of garnet.

The zoning pattern exhibited by the garnets was reversed with Mn-rich rims and Mg,Fe-rich cores. The profiles of FeO, MgO, and MnO are shown in Figure 4.1. Reversely zoned garnets are characteristic of crystal growth under conditions of falling temperature (Allan and Clarke,1981). The Fe/Mg and Fe/(Fe+Mg) ratios were higher in the rims compared to the cores. This relationship is observed even though Fe decreases towards the rim due to the more severe depletion in the MgO near the edge. Similarly, the higher almandine component in the core can be better explained by the low manganese content rather than a significant Fe concentration.

FIGURE 4.1 GARNET PROFILES (GRANITOID)

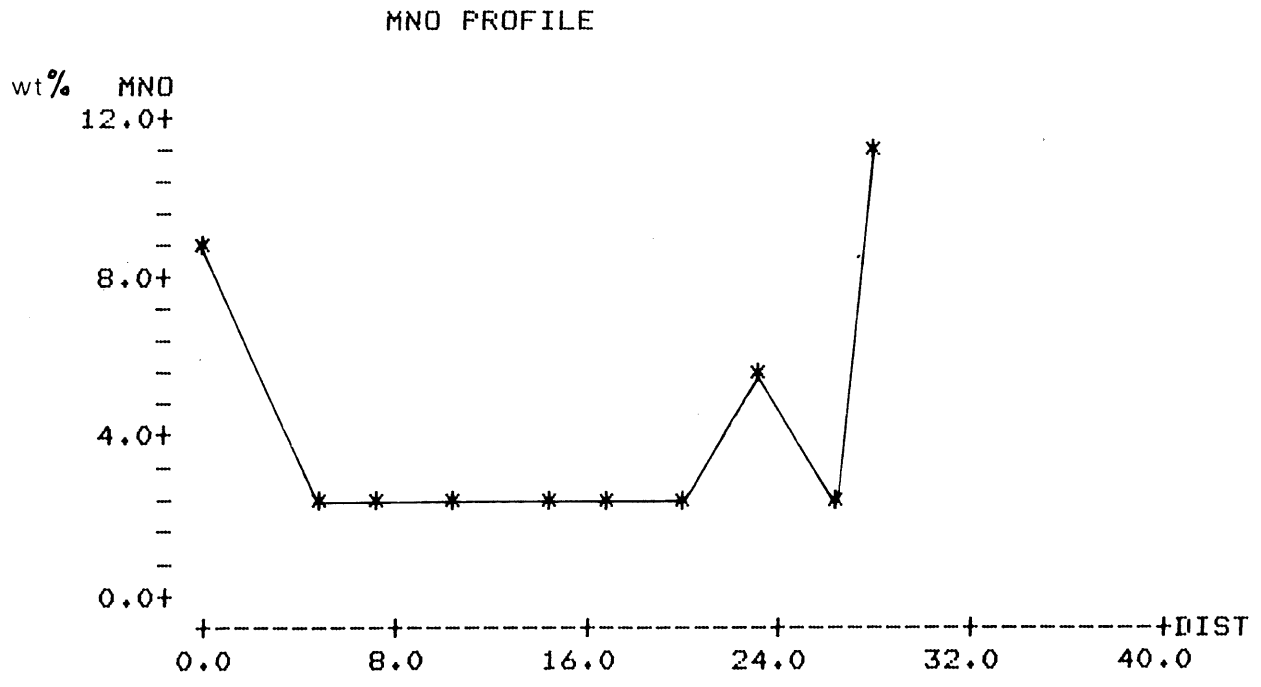
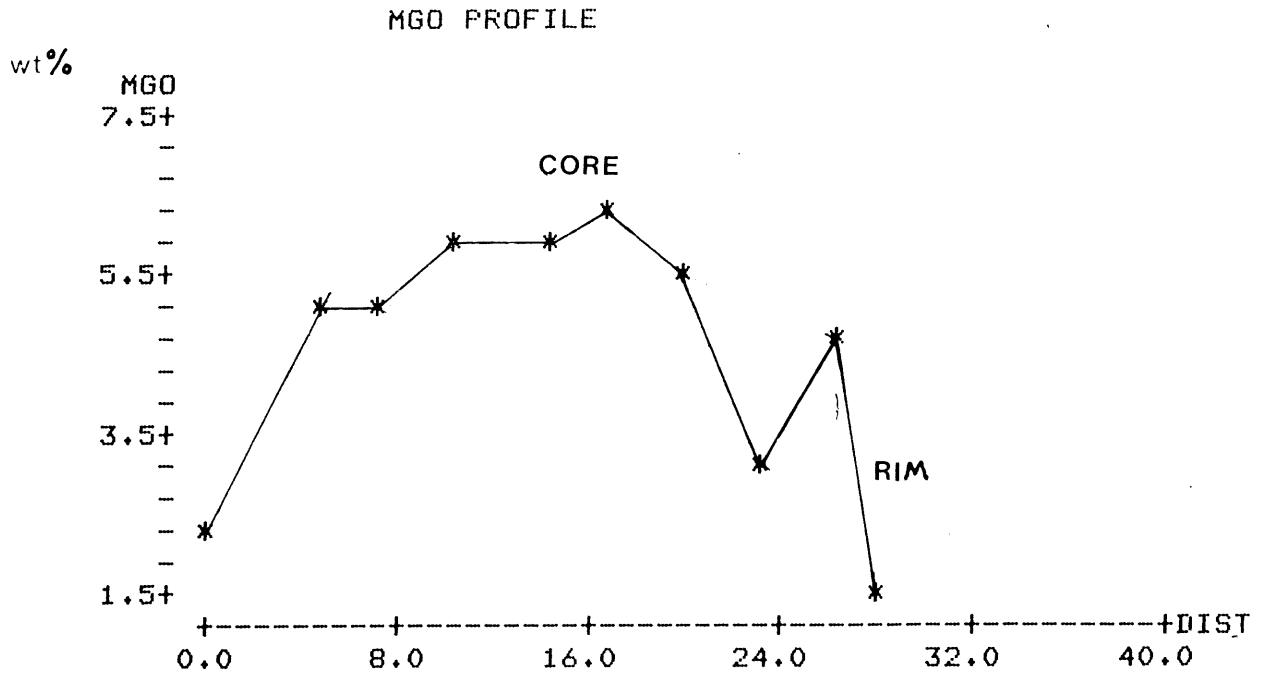


FIGURE 4.1 CONTINUED

FEO PROFILE

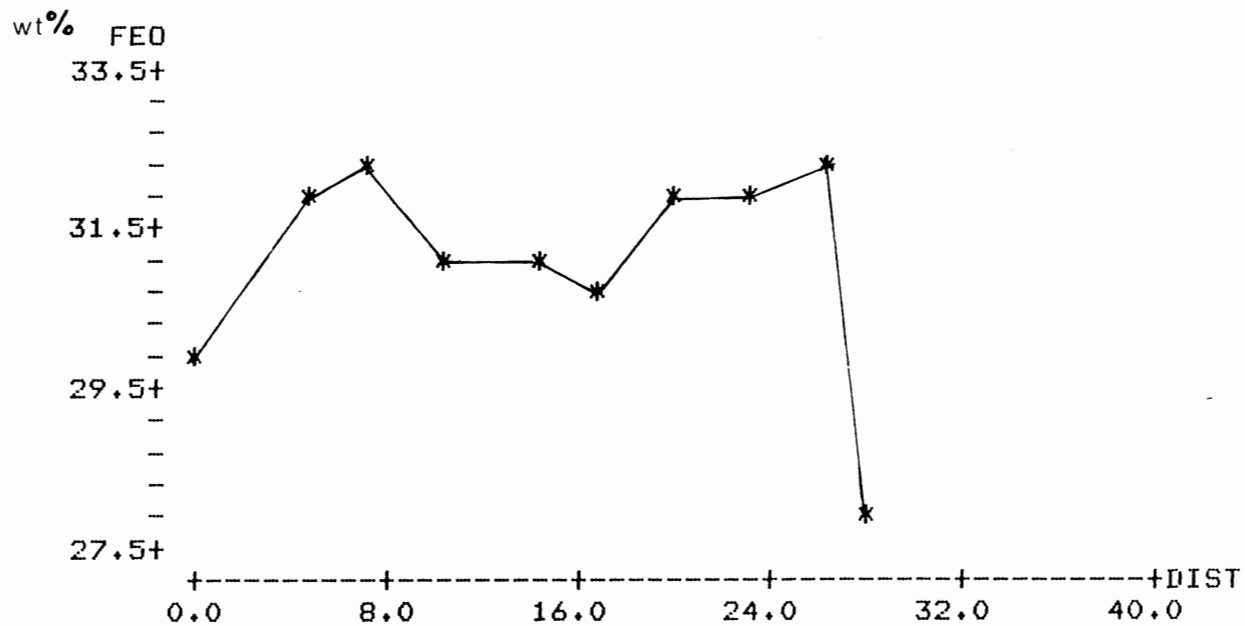


Table 4.1b Meguma Group Garnets (wt %)

Oxide	ZGB-0145 core	ZGB-0191 core	ZGB-0203 core	ZGB-0164 rim	core
SiO ₂	36.55	37.78	36.79	36.73	36.59
Al ₂ O ₃	20.67	20.34	20.86	20.73	20.88
FeO	8.83	22.40	29.64	31.30	29.83
MgO	0.36	0.98	2.49	1.86	1.64
MnO	29.63	11.52	8.21	8.85	10.90
CaO	3.41	6.53	1.79	0.46	0.45
NiO	0.17	--	0.08	--	--
Na ₂ O	0.08	--	--	--	--
TiO ₂	--	0.11	0.07	--	--
Total	99.71	99.60	99.92	99.93	100.29

Oxide	ZGB-0216 core	interm.	rim	core	rim
SiO ₂	37.13	36.58	38.32	37.35	37.01
Al ₂ O ₃	21.19	21.14	20.18	21.01	21.04
FeO	32.49	31.97	31.38	33.72	33.77
MgO	2.76	2.63	2.41	2.91	2.86
MnO	4.80	4.37	4.25	3.55	3.56
CaO	2.14	2.10	1.85	1.87	1.93
K ₂ O	--	--	0.14	--	--
P ₂ O ₅	0.15	0.07	--	--	--
NiO	0.09	--	--	--	--
Total	100.75	98.86	98.53	100.41	100.13

Table 4.1c Granitoid Garnets (wt %)

Oxide	Sample 1 core	rim	Sample 2 core	rim
SiO ₂	37.41	36.74	37.10	36.21
Al ₂ O ₃	21.29	20.81	21.07	20.74
FeO	31.38	28.62	31.81	28.80
Fe ₂ O ₃	1.46	.36	.14	1.32
MgO	5.15	2.26	3.36	2.64
MnO	2.45	8.82	4.10	7.36
CaO	1.33	1.86	1.91	1.85
TiO ₂	0.08	--	--	--
Total	100.50	99.43	99.47	98.79
Fe/Mg	3.843	9.402	6.025	7.958
Fe/(Fe+Mg)	0.794	0.904	0.858	0.888
Spess. Comp	5.53	20.33	9.37	17.21
Alman. Comp	69.34	65.07	71.63	66.46

Table 4.1d Garnet Traverse for Profile (wt. %)

Oxide	312	317	319	322	326
SiO ₂	36.82	37.04	36.98	37.09	37.04
Al ₂ O ₃	20.96	21.16	21.50	21.35	21.38
FeO	30.10	32.02	32.29	30.95	31.09
MgO	2.46	5.20	5.12	5.92	5.78
MnO	8.67	2.33	2.47	2.56	2.37
CaO	1.33	1.26	1.33	1.39	1.36
TiO ₂	--	--	0.06	0.19	0.09
NiO	--	--	--	--	0.06
Total	100.34	99.01	99.75	99.45	99.17

oxide	329	332	335	338	340
SiO ₂	37.68	37.53	36.48	36.79	36.03
Al ₂ O ₃	21.54	21.34	20.70	20.99	20.84
FeO	30.83	31.78	31.73	32.47	27.86
MgO	6.19	5.44	3.29	4.65	1.67
MnO	2.71	2.33	5.26	2.66	11.51
CaO	1.44	1.33	1.19	1.27	0.98
TiO ₂	0.15	0.08	--	--	--
NiO	--	--	--	0.04	--
Total	100.53	99.83	98.65	98.87	98.89

4.2.2 Biotite

Microprobe analysis was done on 11 biotite grains, both metamorphic and magmatic in origin. Thin section ZGB-0300 of the granodiorite contained biotites that were of magmatic origin. The chemical compositions of four biotite grains in the granitoid are shown in Table 4.2a. Two of the grains examined were biotite inclusions in the rim and core of the large garnet in the granitoid. The biotite in the core of the garnet was enriched in Mn and slightly depleted in Fe compared to the biotite inclusion close to the rim. Two analyses were taken of biotites occurring in the groundmass of the granitoid. The Mn content of these biotites fall in

the range of 0.2 to 0.5 wt. %, typical of biotite from felsic igneous rocks. The Al₂O₃ content of the magmatic biotite was above normal, and might be a reflection of the peraluminous nature of the granitoid in Nova Scotia.

Table 4.2a Biotite in Granitoid (wt. %)

Oxide	ZGB-0300			
	gnt rim	gnt core	spot 1	spot 2
SiO ₂	34.38	34.60	34.66	33.60
Al ₂ O ₃	18.88	19.16	18.26	18.17
FeO	23.11	22.99	22.53	23.22
MgO	6.37	6.68	6.30	6.73
MnO	0.40	0.57	0.29	0.46
K ₂ O	9.33	8.63	9.49	8.45
TiO ₂	2.59	2.38	3.51	3.41
CaO	--	0.06	--	--
NiO	--	0.12	--	--
V ₂ O ₅	--	0.15	--	--
Total	95.04	95.39	95.05	94.04

The biotite in the metasedimentary rocks of Meguma Group changed in appearance with increasing grade. In lower grade rocks, the biotite occurred as small flakes, while at higher grades related to thermal metamorphism by the pluton, the biotite formed large, more xenoblastic porphyroblasts. Microprobe analysis was carried out on six grains of metamorphic biotite to determine any variation in chemical composition associated with this transformation. The compositions of these biotites are shown in Table 4.2b. Deer et al. (1972) state that often with increasing grades of metamorphism Fe and Mn decrease, while Ti and Mg increase. To investigate the effects of metamorphic grade, samples ZGB-0133 and ZGB-0216 have been compared, and the results are tabulated in Table 4.2c. Fe and Mn were found

BIOTITE (FEO+MNO-MGO-TIO₂ PLOT)

SYMBOLS

- + MAGMATIC BIOTITE
- ▲ METAMORPHIC BIOTITE

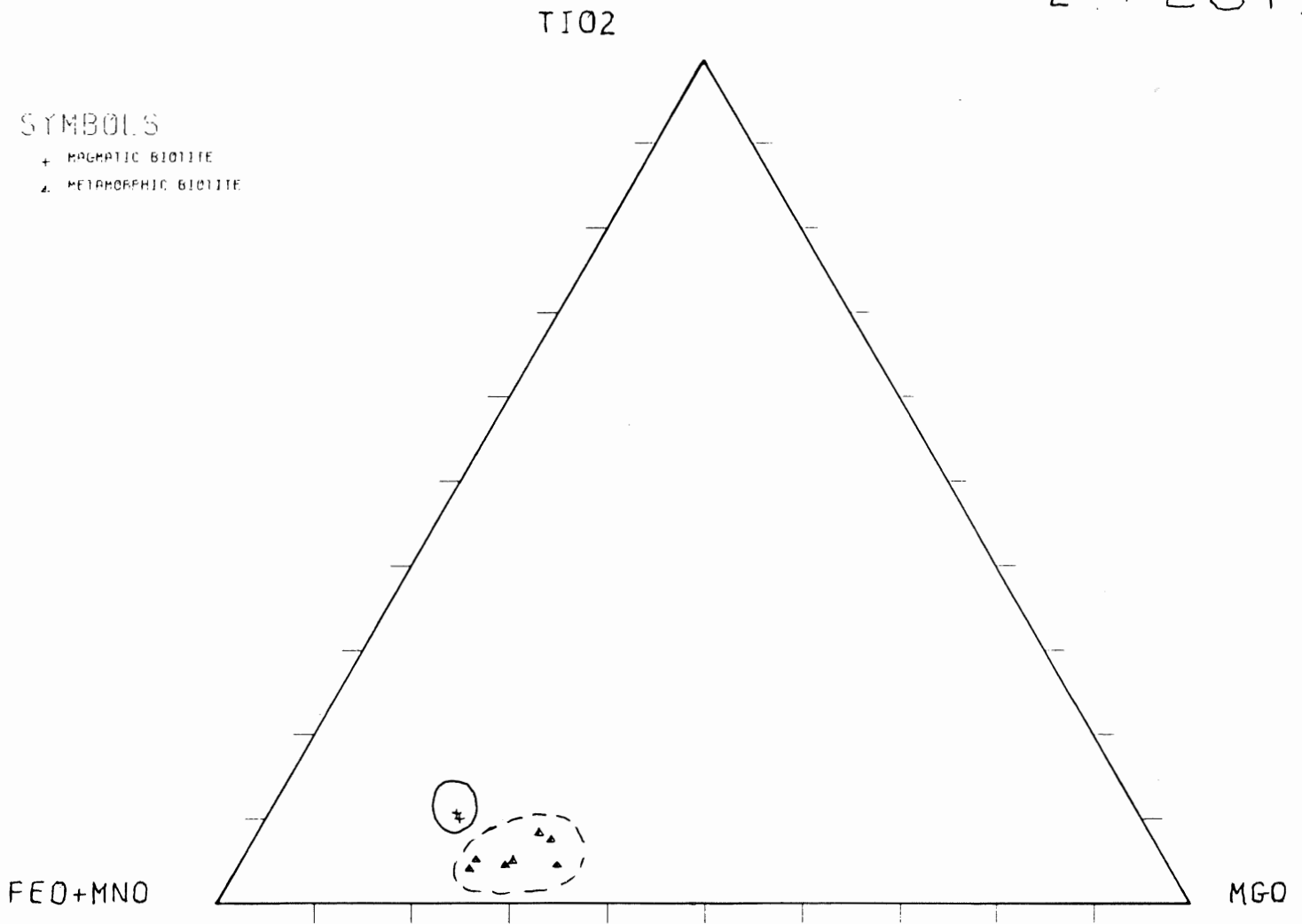


FIGURE 4.2 Triangular diagram showing separation of magmatic biotites of metamorphic biotites.

to decrease, and Mg increased sharply. Ti remained rather constant over the range of grades represented in the rocks. The overall result was a decrease in the Fe/(Fe+Mg) ratio from 0.620 to 0.574 with increased metamorphic grades. Figure 4.2 shows a (FeO+MnO)-MgO-TiO₂ triangular plot of the analyzed biotites. Two distinct groups formed with the magmatic biotites plotting closer to the FeO+MnO corner. The metamorphic biotites show a trend toward increasing Ti and Mg, and decreasing FeO+MnO.

Table 4.2b Biotite in the Meguma Group (wt. %)

Oxide	0133	0142	0191	0164	0260	0216*	0216
SiO ₂	35.29	37.88	36.24	35.34	35.83	34.33	35.03
Al ₂ O ₃	19.54	17.79	20.36	21.23	18.58	20.04	20.62
FeO	21.93	22.47	19.11	20.77	19.37	21.24	18.14
MgO	7.53	7.52	9.97	8.34	8.97	8.86	8.92
MnO	0.16	0.12	0.08	--	0.12	0.14	--
K ₂ O	8.24	6.67	9.00	8.31	9.18	8.22	8.90
TiO ₂	1.60	1.27	1.38	1.37	2.57	1.58	2.19
CaO	--	--	--	0.11	--	--	--
NiO	--	--	--	0.10	--	--	--
CoO	--	--	--	0.09	--	--	--
V ₂ O ₅	--	--	--	0.09	--	--	--
Cr ₂ O ₃	--	--	--	0.08	--	--	--
Na ₂ O	--	--	--	0.11	--	--	--
Cr ₂ O ₃	--	--	--	0.05	--	--	--
Total	94.29	93.71	96.14	95.94	94.62	94.40	93.79

Table 4.2c Chemical Trends in Metamorphic Biotites

	ZGB-0133	ZGB-0216
Mg	1.7329	2.0338
Fe	2.8313	2.7364
Fe/(Fe+Mg)	0.620	0.574
Ti	0.1856	0.1833
Mn	0.0213	0.0185

4.2.3 Chlorite

Seven chlorites from the Meguma rocks and one grain from

the granodiorite were probed, and their chemical compositions are given in Table 4.3a. The metamorphic chlorites were chosen with the hope of representing the different modes of occurrences over the widest range of metamorphic grade. Chlorite was observed to occur as laths defining the foliation, as books crosscutting the foliation, and as large retrograde masses. Chlorite was not seen to be present in thin section ZGB-0216 of the staurolite zone suggesting the discontinuous reaction (Novak and Holdaway, 1981) :

almandine garnet + chlorite + muscovite = staurolite + biotite + H₂O.

Sample 0260 is the chemical composition of chlorite completely replacing a pseudomorph of garnet.

Table 4.3b shows the result of increasing grade on chlorite. The Mg/(Mg+Fe) ratio increases from 0.388 in ZGB-0133 to 0.433 in ZGB-0164, which is the same trend as observed in the biotite. Ionic Mg, Mn and Fe all decreased with increasing grades of metamorphism.

The Mg/(Mg+Fe) ratio in the chlorites of .388 - .433 was somewhat higher than expected. Usually Mg/(Mg+Fe) ratios lower than .25 are thought to favour the formation of staurolite over cordierite at higher grades (Winkler, 1976). Lower pressures are probably involved in the Meguma metamorphic rocks compared to Winkler's example, which would expand the stability field of staurolite on a hypothetical AFM diagram. This allows for the large, idioblastic grains

of staurolite present in the contact aureole.

The chlorite from the granodiorite was very high in Mn compared to most chlorites of igneous origin. The composition of chlorite is often related to that of the original igneous material (Deer et al., 1972), which might mean the granitic magma at Eastville may be enriched in Mn. The magmatic chlorite has abundant Fe in addition to Mn.

Table 4.3a Chlorite Compositions (wt. %)

Oxide	0023	0133	0035	0142	0191	0164	0260	0300
SiO ₂	26.49	27.41	23.77	24.56	26.55	26.57	26.27	24.45
Al ₂ O ₃	25.89	25.70	23.02	23.62	24.10	26.48	19.19	21.53
FeO	22.07	24.88	29.95	29.19	24.37	24.59	30.94	31.43
MgO	11.61	8.86	10.20	10.90	15.45	10.55	11.50	9.87
MnO	0.82	0.41	0.66	0.42	0.28	0.15	0.69	0.71
K ₂ O	0.79	1.49	--	0.07	--	--	--	--
NiO	0.05	--	0.07	--	0.05	0.14	0.05	0.06
TiO ₂	--	--	--	--	0.09	0.12	--	--
V ₂ O ₅	--	--	--	--	--	--	0.15	--
Total	87.22	88.76	87.67	88.76	90.87	88.61	88.81	88.04

Table 4.3b Chemical Trends in Metamorphic Chlorites

	ZGB-0133 (low gnt zone)	ZGB-0164 (garnet zone)
Mg	2.7267	2.6675
Fe	4.2979	3.4894
Mg/(Mg+Fe)	0.388	0.433
Ti	--	0.0153
Mn	0.0720	0.0214

4.2.4 White Micas

White mica was present through the entire range of metamorphism at the Eastville deposit. White mica was a major constituent of the regional metamorphic rocks, and remained stable into the staurolite zone. Microprobe

analysis of three grains has confirmed the white mica to be muscovite (Table 4.4). The chemical analysis showed the white mica to be rich in Al_2O_3 , even for muscovite. TiO_2 increased with metamorphic grade, although Ti tends to be concentrated in biotite over muscovite. The Fe/Mg ratio in the muscovite was found to be 1.720, which is higher than the 1.345 calculated for biotite. It can be seen from this information that the Fe is unequally distributed between the two micas in favour of muscovite.

Table 4.4 White Micas (wt. %)

Oxide	ZGB-0191	ZGB-0164	ZGB-0216
SiO ₂	48.23	46.06	45.73
Al ₂ O ₃	37.20	37.85	36.92
FeO	1.00	0.87	1.10
K ₂ O	10.34	8.20	9.25
Na ₂ O	0.45	1.93	1.33
TiO ₂	0.42	0.25	0.51
MgO	0.60	--	0.36
CaO	0.08	--	0.06
CoO	0.08	--	0.08
MnO	0.06	--	--
V ₂ O ₅	0.24	--	--
Cr ₂ O ₃	0.06	--	--
Total	98.75	95.15	95.34

4.2.5 Oxide Needles

The microprobe was used to identify the oxide opaques in both the granitoid and metamorphic rocks at Eastville. Identification of the oxides was difficult under the microscope, and the probe provided an excellent method of confirmation. The garnet in the granitoid was found to contain inclusions of rutile. Rutile was also present as an accessory mineral in the the metasedimentary rocks. The

grain size of the opaques was so small that contamination from adjacent minerals sometimes crept into the analysis. The chemical compositions of the analyzed oxides are presented in Table 4.5.

Ilmenite was the more abundant oxide present in the metamorphic rocks. They occurred as very small, elongate needles, and often defined the foliation. With increasing grade the MnO content of the ilmenites decreased, while the FeO content increased. The ilmenites may be important as a source for the manganese contained in the spessartine garnets.

Table 4.5 Oxide Needles (wt. %)

Oxide	Ilmenite				Rutile		
	0133	0164	0164	0158	0164	0300	0300
TiO ₂	51.82	51.08	48.44	53.82	91.96	96.33	97.91
FeO	40.43	44.16	42.29	45.15	2.20	0.18	--
MnO	6.43	1.49	2.17	2.13	--	0.19	0.17
SiO ₂	1.06	0.20	1.87	--	0.91	0.58	--
Al ₂ O ₃	0.23	0.15	1.56	--	0.68	0.48	--
K ₂ O	0.06	0.07	0.51	--	0.14	0.22	0.07
V ₂ O ₅	--	--	0.13	--	0.19	--	0.34
CaO	--	--	0.09	--	--	--	0.10
MgO	--	--	--	0.06	--	0.13	--
CoO	--	--	--	--	--	0.04	0.10
Total	100.02	97.14	97.08	101.16	96.09	98.16	98.84

4.2.6 Staurolite

Large porphyroblasts of staurolite were present in thin section ZGB-0216. The staurolite forms light yellow, idiomorphic grains with a sieve texture. The staurolite in this slide appeared very fresh in comparison to other staurolite in samples in the vicinity. The assemblage in

this rock marks the highest grade of metamorphism observed at Eastville. Staurolite most commonly forms in rocks of high Fe/(Fe+Mg). The chemical compositions of staurolite analyzed on the microprobe are given in Table 4.6. The analyses showed the composition to be extremely uniform throughout the slide. The Fe/(Fe+Mg) ratio in the staurolite was 0.842.

Table 4.6 Staurolite (wt. %)

Oxide	Sample 1	Sample 2	Sample 3
SiO ₂	27.05	27.19	27.65
Al ₂ O ₃	54.09	54.39	53.70
FeO	13.91	13.93	14.45
MgO	1.17	1.38	1.52
MnO	0.28	0.29	0.24
TiO ₂	0.59	0.53	0.48
CoO	0.07	--	0.04
K ₂ O	0.05	--	--
V ₂ O ₅	--	0.09	--
NiO	--	0.12	--
Total	97.22	97.92	98.09

4.2.7 Andalusite

Andalusite occurs as large porphyroblasts often localized to the graphitic layers of the Halifax slate. It was thought that the andalusite may contain MnO originating from the contorted bed of the Meguma Group. Microprobe analysis showed that no such enrichment occurred. The compositions of the two analyzed grains, which are presented in Table 4.7, were uniform, and dominated by the alumina and silica constituents.

Table 4.7 Andalusite (wt. %)

Oxide	ZGB-0158	
	Spot 1	Spot 2
Al ₂ O ₃	61.61	61.94
SiO ₂	36.05	35.93
K ₂ O	0.07	0.10
FeO	0.14	0.23
NiO	--	0.10
CaO	--	0.05
V ₂ O ₅	--	0.07
Total	97.87	98.42

4.2.8 Plagioclase in the Granitoid

Three plagioclase crystals from the granodiorite were analyzed by the microprobe, and the results are shown in Table 4.8. From petrographic observation the Michel-Levy method gave a plagioclase composition of An₃₀. The microprobe analysis confirmed the andesine composition of the plagioclase.

Table 4.8 Plagioclase in Granitoid (wt. %)

Oxide	ZGB-0300		
	Spot 1	Spot 2	Spot 3
SiO ₂	61.90	59.31	60.04
Al ₂ O ₃	23.61	25.26	24.69
Na ₂ O	8.71	7.51	7.93
K ₂ O	0.34	0.26	0.24
CaO	5.22	7.25	6.63
CoO	0.05	--	0.06
FeO	--	0.04	--
Cr ₂ O ₃	--	0.06	0.06
V ₂ O ₅	--	--	0.08
Total	99.81	99.70	99.73

4.3 Discussion

The results of the microprobe analyses have raised some interesting questions. The garnets in the granitoid and metamorphic rocks showed different zoning patterns. Garnet

in the granodiorite displayed reverse zoning, while the zoning pattern in the garnet of the Meguma Group was 'normal'.

In progressive metamorphic terrains, Mn tends to be concentrated in the cores of the garnet governed by the distribution coefficient K_D . The assumptions involved in the normal zoning models are equilibrium conditions, perfect diffusion in the matrix surrounding the garnet, and negligibly slow growth of the crystal (Jamieson, 1974). The zoning pattern described in the Meguma Group garnets can be considered typical of garnets of a progressive metamorphic origin.

The reversed zoning reflected in the profiles of Figure 4.1 suggests one of two origins for the garnet in the granodiorite, a magmatic type or a highly modified xenolithic type. A highly modified xenolithic garnet would not fulfill the conditions of the models suggested for normal zoning. The immersion of the garnet in the high temperature environment of the magma would cause rapid crystallization. A manganese-depleted zone forms when diffusion of Mn cannot keep up with the rapid growth of the garnet (Edmunds and Atherton, 1971). As the growth rate of the garnet decreases with time, equilibrium would be re-established, and manganese would be supplied to the grain boundary according to the ideal distribution. This accounts for the Mn-rich rims observed in the garnet profiles. Other lines of evidence supporting a metamorphic origin are the

presence of pyrite adjacent to the garnet in the granodiorite, inclusions of biotite and muscovite, and the small quantity of grains.

Magmatic garnets are not a common occurrence in igneous rocks, but the controversy over their origin has stimulated much interest in this field. The most common occurrence of magmatic garnets is in felsic, peraluminous granitoid rock. Magmatic garnets are typically euhedral, inclusion poor or inclusion free, and essentially almandine-spessartine solid solutions (Miller and Stoddard, 1981). The compositions of garnets and coexisting mafic minerals suggest that magmatic garnets crystallize in environments with unusually high Mn/(Fe + Mg) ratios. Other studies have shown that garnets found in granitoids contain >10% spessartine component. Biotites coexisting with these garnets have higher MnO, >.75 wt.% compared to 0.2% of average biotites in igneous rocks without garnets. Miller and Stoddard (1981) conclude that most granitoid garnets crystallize from manganese rich, peraluminous magmas. Experimental work (Green, 1978) shows that high Mn in magmas increases the stability of garnet permitting crystallization at pressures of 3 kb or less.

Turning to this study, a case exists for a magmatic origin of the garnets in the granodiorite at Eastville. The granitoid complex is peraluminous, and most of the garnets tend to be inclusion poor, almandine-spessartine solid solutions. The spessartine component of the garnets in the granodiorite varies from the core to the rim. The core has

an average spessartine component of 7.5%, while the rim shows a higher spessartine component at almost 19%. Although the MnO content of coexisting biotite in the granodiorite is 0.29%, chlorite is greatly enriched in MnO at 0.71 wt.%. It might be speculated that the Mn enrichment, if existent, in the granitic magmas at Eastville occurred due to the assimilation of the Mn-rich sediments of the Meguma Group.

The triangular plot of metamorphic biotites at Eastville showed a trend towards decreasing (FeO+MnO) and increasing TiO₂ and MgO. This trend can be explained by the incorporation of Fe into the higher grade metamorphic minerals such as garnet and staurolite. Chlorite shows the same chemical characteristics of losing its Fe to these iron-rich minerals. The thermal influence of the pluton in the east has left Domain III relatively barren of Mn. Mn is abundant in the regional metamorphic rocks of the west, but this zone gives way to the contact aureole containing metamorphic minerals showing depleting Mn contents. Garnet, biotite, and chlorite in the east all contain less Mn than their counterparts in the west. Under extreme metamorphic conditions Mn seems to be dispersed rather than concentrated in economic quantities.

Chapter 5 : Pressure-Temperature Conditions

5.1 General Statement

Petrological studies have become increasingly concerned with the quantitative estimation of the conditions of metamorphism. Over the last number of years experimental data have accumulated on various systems defining the conditions under which a phase assemblage is at stable equilibrium. On a petrogenetic grid each mineral assemblage falls in a unique P-T domain immediately conveying the conditions of metamorphism. More recently activity-composition relationships have achieved a good measure of consistency in certain systems between theory, experiments and observations, and provides the basis for geothermobarometry. Both the petrogenetic grid and geothermometry approaches are here used in an attempt to determine the temperature-pressure conditions of the metamorphic events affecting the Meguma Group at Eastville.

5.2 Mineral Assemblages

5.2.1 Regional Metamorphic Conditions

The most common regional metamorphic assemblage observed in Domain I is quartz + muscovite + spessartine garnet + chlorite + plagioclase. This corresponds to the quartz-albite-muscovite-chlorite subfacies of the greenschist facies of Turner and Verhoogen (1960). They

have estimated that metamorphism of the greenschist facies sets in over a range of temperature originating at close to 300 ° C. The upper temperature limit of the regional metamorphic event at Eastville may be set at the temperature biotite enters the system. Winkler (1974) presents experimental data by Nitsch which shows temperatures of 445° C at 4 kb and 460° C at 7 kb are needed before biotite will form. Spessartine garnet is abundant in the regional metamorphic assemblage at Eastville, and is stable at much lower temperatures and pressures than almandine garnet. Mn-chlorite converts to spessartine garnet at temperatures between 370 and 420° C at relatively low pressures. It is evident from this discussion that the temperature of regional metamorphism during the Acadian orogeny was between 370 and 430° C. The pressure estimates for this deformation encompasses a large range, anywhere from 3 to 8 kb are possible.

5.2.2 Contact Metamorphic Conditions

The highest grade assemblage observed in the contact zone at Eastville was staurolite + almandine garnet + biotite + muscovite + quartz. Hoschek (1969) found the equilibrium conditions of the reaction :

chlorite + muscovite = staurolite + quartz + biotite + H₂O
are 565±15° C at 7 kb and 540±15° C at 4 kb. The maximum stability of staurolite in the presence of quartz, muscovite, and biotite was measured at 675±15° C at 5.5 kb

and $575 \pm 15^\circ\text{C}$ at 2 kb. The more common assemblage of almandine garnet + biotite + chlorite + muscovite + quartz + andalusite is thought to be stable at temperatures above 500°C at 4 kb and 600°C at 5 kb. Andalusite porphyroblasts in lower medium grade assemblages adjacent to the pluton indicate that during emplacement the pressure was definitely less than 6 kb, and probably closer to 4 kb (Holdaway, 1971).

5.3 Garnet-Biotite Geothermometry

The presence of coexisting biotite and garnet in the contact metamorphic rocks at Eastville allows the use of a geothermometer based on Fe-Mg partitioning. The basis of the garnet-biotite geothermometer is that the distribution coefficient (K_D) of Fe-Mg partitioning is independent of pressure and $a_{\text{H}_2\text{O}}$. The chemical composition of the rim, core, and an intermediate position of the garnet was measured using the microprobe. A biotite in mutual contact with this garnet was also probed for its composition. An assumption made is that the core of the garnet equilibrated with the coexisting biotite of the same composition as now present in the rock. From the microprobe data it is necessary to compute the mole fraction ratio of Fe to Mg for both biotite and garnet. The distribution coefficient is just the mole fraction ratio of Fe to Mg for garnet divided by that for biotite.

Theoretical arguments and temperature estimates from

other sources allowed Thompson (1976) to calibrate a linear relationship of $\ln K_D$ to reciprocal temperature for garnet-biotite pairs. Perchuk (1977) has used the amphibole-garnet geothermometer to estimate the effect of temperature on Fe-Mg partitioning in the garnet-biotite system. Ferry and Spear (1978) conducted experiments with synthetic phases at 2.07 kbar and 550-800°C to determine a relationship between $\ln K_D$ and temperature. The estimated temperatures of formation using these three independent calibrations are shown in Table 5.1. The temperatures of Thompson, and Ferry and Spear incorporate errors of ± 50 C, while Perchuk does not state his expected error.

Table 5.1 Geothermometry Data

Sample	Mineral	Fe/Mg	Kd	T1(°C)	T2(°C)	T3(°C)
ZGB-0216	Garnet core	6.6107	4.915	615	611	604
	Gnt interm.	6.8233	5.073	603	602	597
	Garnet rim	7.3020	5.429	579	584	583
	biotite	1.3455				

T1 = Ferry and Spear (1978). T2 = Thompson (1976). T3 = Perchuk (1977).

The garnet-biotite geothermometer assumes a pure binary system, and caution should be exercised in applying the results to systems containing significant amounts of Mn and Ca in garnet, and Al(VI) and Ti in biotite. The MnO content of the almandine garnets is the major concern due to the abundance of Mn in the sediments of the Meguma Group at Eastville. The almandine garnets from the staurolite zone of the contact aureole had a range of MnO content from 4.25

- 4.80 wt. %. The agreement of the calculated temperatures with the petrogenetic grid determination suggest that the contents of the minor phases are small enough to allow the relationship between K_D and T to apply.

The temperatures from the three calibrations all gave temperatures reasonably close to each other. The temperatures acquired from the garnet rim and biotite calculation are considered best as this is when the two minerals are most likely in equilibrium. From this investigation it can be said that the temperature reached in the contact aureole was approximately 580°C.

Chapter 6: General Discussion

6.1 Relative Age of the Mineralization

Five possibilities exist to explain the origin of Pb-Zn in the metasedimentary rocks at Eastville. These possibilities are outlined as follows : 1) syngenetic; 2) diagenetic; 3) regional metamorphic; 4) related to the granitoid pluton; and 5) post granite. A syngenetic origin would involve precipitation of the ore minerals at the same time as the deposition of the sediments. Diagenesis implies formation of the sulphides after the deposition of the sediments but before their consolidation into rocks. A regional metamorphic origin suggests concentration of the Pb and Zn sulphides by metamorphic processes. The Pb and Zn may have its source in the granite, and be introduced into the country rock during its emplacement. Lastly, the Pb-Zn may have been introduced in some post-granitic process, such as shearing in the Hercynian Orogeny.

Textural evidence from this study poses some constraints on possible genetic hypotheses. Sphalerite occurring in the core of some regional metamorphic spessartine garnets indicates that the mineralization was present prior to the regional metamorphism associated with the Devonian Acadian Orogeny. Clearly a hypothesis suggesting a late introduction of the Zn and Pb into the Meguma strata can now be rejected. Thus the hypotheses involving introduction of the base metals directly from the granitoid or from an even

later event can be ruled out. A regional metamorphic origin can be discarded because sphalerite had to be present for the spessartine garnet to nucleate around it. Two hypotheses remain to be considered.

It is tempting to consider the Eastville deposit as a sediment-hosted stratiform lead-zinc deposit in view of the relatively old (that is, pre-metamorphic) age suggested for the introduction of Pb and Zn into the Meguma host. The characteristics of stratiform lead-zinc deposits are described by Large (1983), and some are applicable to the Eastville deposit. The mineralized area is laterally extensive (over 10 km in length), and restricted to a thin part of the complete stratigraphic section. This agrees with the morphology of these types of deposits which have lateral dimensions an order of magnitude greater than their thickness. The independent distribution of iron and manganese from the zinc-lead minerals, the association with graphitic black slates, and the presence of sphalerite in the cores of the spessartine garnet are compatible with the model proposed by Large (1983) for stratiform lead-zinc deposits. However, the lack of metal zonation in a geographic and stratigraphic sense, and the predominance of remobilized sphalerite and galena over that of 'sedimentary' Pb-Zn sulphides makes the Eastville deposit distinct from this hypothesis. No evidence of penecontemporaneous igneous activity has been found which would be an indication of a

high geothermal gradient necessary for the convective circulation of fluids in the deposited sediments.

The relative scarcity of sphalerite in the cores of the garnet suggests that the Zn was still mobile prior to the regional metamorphic event. This would seem to favour the diagenetic hypothesis as diagenesis involves a wider range of physicochemical conditions than the synsedimentary hypothesis. The diagenetic hypothesis is not restricted to one set of conditions, and thus allows a better explanation of the occurrence of both Pb-Zn and Mn. Most of the Fe-sulphides would have formed by reduction of iron in the carbonaceous sediment as an early diagenetic event.

6.2 Metamorphism at Eastville

In the geological history of Eastville, regional metamorphism and structural events associated with the Acadian Orogeny followed the deposition of the Meguma sediments. Regional metamorphism reached the lower greenschist facies resulting in recrystallized quartz, and the formation of chlorite, muscovite and spessartine garnet. Temperature estimates for this event are in the range of 370 to 420°C. The high manganese content of the sediments is reflected in the formation spessartine garnets, and to a lesser degree, ilmenite and calcite. During this period of metamorphism pyrite was in part converted to pyrrhotite. The metasedimentary rocks of the Meguma Group were compressed into a series of anticlines and synclines during

the Acadian Orogeny. The Eastville deposit is located on the northern limb of one of these synclines. Faults were active during this time, which associated with the regional metamorphism redistributed some of the ore minerals into cross cutting veinlets and fracture systems.

The Eastville deposit was truncated in the east by a granitoid pluton. Contact metamorphism further changed the minerals of the Meguma Group rocks in the contact aureole. An assemblage of almandine garnet + biotite + andalusite + staurolite + chlorite + quartz + muscovite was developed in the metasedimentary host. The temperature of this stage of metamorphism was determined by garnet-biotite geothermometry to be in the area of 580°C. Once again the base metals were susceptible to mobilization due to the high temperatures and fracturing associated with the emplacement of the granite.

6.3 Late Remobilization

Topographic lows in the Meguma basement were filled with marine carbonate and sulphate, and subaerial clastics of the Carboniferous Windsor Group. It has been suggested that the Meguma Group could be the source for base metals remobilized into the Carboniferous sedimentary cover (Akande and Zentilli, 1984). The evidence supporting this suggestion is preliminary Pb isotope data that indicates the age of the Pb in the carbonate-hosted Pb-Zn deposits at Gays River, Walton, and Pembroke is around 450 m.y. (Ordovician).

Tectonism in the form of regional faulting and shearing

was severe in Nova Scotia during the Late Carboniferous. Poole (1967) recognized this period of deformation, and called it the Maritime Disturbance. Deformation in the Devonian-Carboniferous plutons are probably a reflection of this increased tectonic activity. This intrusive and/or thermotectonic event (Reynolds et al., 1981) provided suitable conditions for the Pb in the Meguma Group to be remobilized into the Carboniferous basins. Heat associated with the deformation would mobilize the metals, while the extensive faulting would create pathways for its movement. Fluids might be present from dehydration reactions involved in the thermal event. Excess metamorphic pore fluid pressure may further induce fracturing, increasing the permeability in the rock to allow easier passage of the mineralizing fluids. The genesis of the carbonate-hosted Pb-Zn deposits is currently under study, and should provide more details on their formation (Ravenhurst, 1984).

6.4 Interaction of the Granitoid and Meguma Metasediments

The interaction between these two rock bodies can be viewed in two ways. The granitoid pluton influenced the mineralogical-geochemical nature of the Meguma rocks; and by the nature of the emplacement of the granitoid body, the Meguma could possibly have affected the mineralogical and chemical characteristics of the granite.

The effect of the pluton on the Meguma has already been discussed in other sections. The economic mineralization

would be metamorphosed, and possibly remobilized by the heat from the granite. The common rock forming minerals of the Meguma rocks underwent significant changes associated with this thermal event as well. In regards to carbonate, which is abundant in the regional metamorphic domain in the west, it is absent from the from the contact assemblage. The Ca from the breakdown of the calcite probably went into the plagioclase and almandine garnet of the contact zone. The plagioclase should show an increased anorthitic component in the contact zone if this is the case. This was not tested. The Fe and Mn contents of metamorphic biotite and chlorite dropped with higher grades of metamorphism, with these cations going into the making of Fe-rich minerals such as staurolite and almandine garnet. No evidence has been found through this study to suggest any large scale (several km) metasomatic event.

The metasedimentary rocks of the Meguma Group have a much more subtle affect on the granitoid pluton. The evidence for assimilation of the Meguma rocks includes the observation of rounded xenoliths in the granite, the presence of garnets in the granodiorite as an accessory mineral which may be metamorphic in origin, and the occurrence of pyrite in the granite most probably originating from the country rock. The degree of assimilation of the metasedimentary rock is difficult to quantify with the use of our chemical data. Enrichment of zinc in the granitoid pluton at Eastville exists, but it is

not significantly higher than the Zn content of the South Mountain Batholith. The Pb:Zn ratio of the pluton at Eastville is almost identical to the Pb:Zn ratio of 1:2.2 shown in the Meguma rocks. The Pb:Zn ratio of various plutons of the South Mountain Batholith ranges from 1:.613-.833 (Smith,1979), thus substantially higher than Hattie Lake Pluton. It is possible to speculate that the Pb:Zn ratio in Hattie Lake Pluton may be inherited from the assimilated Meguma rocks.

Chapter 7 : Conclusions

1) The presence of sphalerite in the cores of the regional metamorphic spessartine garnets establishes that the mineralization was prior to both the ~~the~~ emplacement of the granitoid pluton, and the deformation associated with the Acadian orogeny.

2) Based on this textural evidence, the mineralization at Eastville cannot be related directly to the granitoid body or some later event, or cannot have formed through metamorphic processes. A syngenetic or diagenetic origin better explains the base metal mineralization of the Eastville deposit.

3) The trace element chemistry of Hattie Lake Pluton shows it to be a comagmatic, differentiated suite of granitic rock possessing similar differentiation trends as the South Mountain Batholith.

4) Regional metamorphism in the Meguma rocks at Eastville was to the lower greenschist facies due to an observed mineral assemblage of chlorite + spessartine garnet + muscovite + quartz. Temperature estimates according to this assemblage are from 370°C to 400°C.

5) The temperature achieved in the contact aureole was estimated by garnet-biotite geothermometry to be around 580°C, which agreed with a temperature obtained using the

mineral assemblage of staurolite + almandine garnet + biotite.

6) With increasing grades of metamorphism, the Mn content in biotite, garnet, and chlorite in the contact zone was found to decrease.

Chapter 8 : Recommendations

- 1) The asymmetrical distribution of carbonate over the length of the deposit cannot be explained from this study. It is suggested that microprobe analysis of the plagioclase may explain where the Ca is taken up during higher grades of metamorphism.
- 2) In an effort to obtain more evidence for the assimilation of the Meguma metasediments into the pluton, sulfur isotopes might be used to determine whether pyrite in the granitoid is metamorphic with a sulphur ratio characteristic of the Meguma.
- 3) More petrographic studies of the ore minerals should be undertaken to determine how commonly the garnets nucleated around the mineralization.
- 4) A sedimentological study of the the Eastville deposit would lead to a better understanding of the distinct lithologies in respect to turbidite deposition.
- 5) A structural study of the Eastville deposit should be initiated to evaluate the syngenetic hypothesis with respect to a feeder zone.
- 6) Geothermometry might be tried on the ore mineralization to see if the ore records similar thermal events as the silicate rocks.

References

- Akande, S.O. and Zentilli, M. (1984) Geologic, Fluid Inclusion, and Stable Isotope Studies of the Gays River Lead-Zinc Deposit, Nova Scotia, Canada. *Economic Geology*, vol.79, pp. 1187-1211.
- Allan, B.D. and Clarke, D.B. (1981) Occurrence and Origin of Garnet in the South Mountain Batholith, Nova Scotia. *Canadian Mineralogist*, vol.19, pp. 19-24.
- Benson, D.G. (1967) Geology of the Hopewell map area, Nova Scotia; Geological Survey of Canada, Memoir 343, 58p.
- Binney, W.P., Jenner, K.A., Sangster, A.L., and Zentilli, M. (in press) A Stratabound zinc-lead Deposit in Meguma Group Metasediments at Eastville, Nova Scotia.
- Binney, W.P. (1981) Gold Brook - Report on 1980 Till Drilling and Drill Core Analysis, Confidential Report for St. Joseph Explorations Ltd.
- Chatterjee, A.K. and Strong, D.F. (1984) Rare Earth and Other Element Variation in Greisens and Granites Associated with East Kemptville Tin Deposit, Nova Scotia, Canada. *Transactions of the Institution of Mining and Metallurgy, Section B*, vol. 93, pp. B59-B70.
- Clarke, D.B. and Halliday, A.N. (1980) Strontium Isotope Geology of the South Mountain Batholith, Nova Scotia. *Geochimica et Cosmochimica Acta*, vol. 44, pp. 1045-1058.
- Deer, W.A., Howie, R.A., and Zussman, J. (1972) *An Introduction to the Rock Forming Minerals*. Longman Group Ltd., London, 527 pp.
- Edmunds, W.M. and Atherton, M.P. (1971) Polymetamorphic Evolution of Garnet in the Fanad Aureole Donegal, Eire. *Lithos*, vol.4, pp. 147-161.
- Fairbairn, H.W., Hurley, P.M., Pinson, W.H. Jr., and Cormier, R.F. (1960) Age of Granitic Rocks of Nova Scotia. *Geological Society of America Bulletin*, vol. 71, pp. 399-414.
- Ferry, J.M. and Spear, F.S. (1978) Experimental Calibration of the Partitioning of Fe + Mg Between Biotite and Garnet. *Contributions to Mineralogy and Petrology*, vol.66, pp. 113-117.

- Fletcher, H. and Faribault, E.R. (1903) Eastville sheet no.48; Geological Survey of Canada, Map 633.
- Fyson, W.K. (1966) Structures in the Lower Paleozoic Meguma Group, Nova Scotia. Geological Society of America Bulletin, vol. 77, pp. 931-944.
- Geological Survey of Canada (1960) Aeromagnetic Map 762G, Hopewell, Nova Scotia.
- Graves, M.C. and Zentilli, M. (1982) A Review of the Geology of Gold in Nova Scotia. Geology of Canadian Gold Deposits, Special Volume 24, pp 1-10.
- Green, T.H. (1978) Garnet in Silicic Liquids and Its Possible Use as a P-T Indicator. Contributions to Mineralogy and Petrology, vol 65, pp59-67.
- Harris, I.M. and Schenk, P.E. (1975b) The Meguma Group (Lower Paleozoic, Nova Scotia). Maritime Sediments, vol. 11, pp. 25-46.
- Holdaway, M.J. (1971) Stability of Andalusite and the Aluminum Silicate Phase Diagram. American Journal of Science, vol. 271, pp. 97-131.
- Hoschek, G. (1969) The Stability of Staurolite and Chloritoid and Their Significance in Metamorphism of Pelitic Rocks. Contributions to Mineralogy and Petrology, vol.22, pp. 208-232.
- Jamieson, R.A.(1974) The Contact of the South Mountain Batholith Near Mt. Uniacke, Nova Scotia, B.Sc. thesis, Dalhousie University, Halifax, Nova Scotia.
- Jenner, K.A. (1982) A Study of Sulphide Mineralization in the Meguma Group sediments, Gold Brook, Colchester County, Nova Scotia, B.Sc. thesis, Dalhousie University, Halifax, Nova Scotia.
- Large, D.E. (1983) Sediment-Hosted Massive Sulphide Lead-Zinc Deposits: an Empirical Model. In Short Course in Sediment Hosted Stratiform Lead - Zinc Deposits, eds.D.F. Sangster, Mineralogical Association of Canada, pp. 1-30.
- Liew, M. (1979) Geochemical studies of the Goldenville Formation at Taylor Head, Nova Scotia. M.Sc. thesis, Dalhousie University, Halifax, Nova Scotia.
- Lowdon, J.A., Stockwell, C.H., Tipper, H.W., and Wanless, R.K. (1963) Age Determinations and Geological Studies (including isotopic ages - Report 3). Geological Survey

of Canada, Paper 62-17.

- MacInnis, I. (1984) A Stable Isotope Study of Carbonates Within the Manganiferous Zn-Pb Deposit at Eastville, Nova Scotia. Dalhousie University CO-OP Program, Departments of Chemistry and Geology, Internal Report, Year 4, Work Term 2, 46 pp.
- MacInnis, I. (1983) A Geological and Geochemical Study of the Halifax - Goldenville Contact in the Meguma Group of Nova Scotia. Dalhousie University CO-OP Program, Departments of Chemistry and Geology, Internal Report, Year 3, Work Term 1, 77 pp.
- McKenzie, C.B. and Clarke, D.B. (1975) Petrology of the South Mountain Batholith, Nova Scotia. Canadian Journal of Earth Sciences, vol. 12, pp.1209-1218.
- Miller, C.F. and Stoodard, E.F. (1981) The Role of Mn in the Paragenesis of Magmatic Garnet : An Example From the Old Woman Piute Range, California. Journal of Geology, vol. 89, pp. 233-246
- Novak, J.M. and Holdaway, M.J. (1981) Metamorphic Petrology, Mineral Equilibria and Polymetamorphism in the Augusta Quadrangle, south-central Maine. American Mineralogist, vol.19, pp 19-24.
- Perchuk, L.L.(1977) Thermodynamic Control of Metamorphic Processes. In Saxena, S.H. and Bhattacharji, S. (Eds.) Energetics of Geological Processes, pp.285-332, Springer-Verlag.
- Poole, W.H. (1967) Tectonic Evolution of Appalachian Region of Canada. In Geology of the Atlantic Region (Eds.) E.R.W Neale and H. Williams, Geological Association of Canada, Special Paper 4, pp. 9-51.
- Poole, W.H. (1971) Graptolites, Copper, and Potassium-argon in Goldenville Formation, Nova Scotia. In: Report of Activities, R.G. Blackadar (Ed.). Geological Survey of Canada, Paper 71-1A, pp. 9-11.
- Ravenhurst, C. (1984) Discussion of Models for the Formation of Mississippi Valley Type Deposits as They May Apply to the Carboniferous basins of Nova Scotia, (abs), Maritime Sediments and Atlantic Geology, vol.20
- Reynolds, P.H., Kublick, E.E., and Muecke, G.K. (1973) Potassium-Argon Dating of the Slates from the Meguma Group, Nova Scotia. Canadian Journal of Earth Sciences, vol. 10, pp. 1059-1067.

- Reynolds, P.H., Zentilli, M., and Muecke, G.K. (1981) K-Ar and Ar/Ar Geochronology of Granitoid Rocks from Southern Nova Scotia : Its Bearing on the Geological Evolution of the Meguma Zone of the Appalachians. Canadian Journal of Earth Sciences, vol. 18, pp. 386-394.
- Schenk, P.E. (1978) Synthesis of the Canadian Appalachians. Geological Survey of Canada, Paper 78-13, pp. 111-136.
- Schenk, P.E. (1970) Regional Variation of the Flysch - Like Meguma Group (Lower Paleozoic) of Nova Scotia compared to Recent sedimentation off the Scotian Shelf. Geological Association of Canada, Special Paper 7, pp. 127-153.
- Sivraprakash, C. (1981) Zoned Garnets in Some Scottish Dalradian Pelites. Mineralogical Magazine, vol 44 , pp. 301-307.
- Smith, T.E. (1979) The Geochemistry and Origin of the Devonian Granitic Rocks of Southwest Nova Scotia. Geological Society of America Bulletin, vol. 90 (II), pp.850-885.
- Taylor, F.C. and Schiller, E.A. (1966) Metamorphism of the Meguma Group of Nova Scotia. Canadian Journal of Earth Sciences, vol. 3, pp 959-974.
- Taylor, S.R. (1965) The Application of Trace Element Data to Problems in Petrology. Physics and Chemistry of the Earth, vol. 6, pp. 133-213.
- Thompson, A.B. (1976) Mineral Reactions in Pelitic Rocks II. Calculation of Some P-T-X(Fe-Mg) Phase Relations, American Journal of Science, vol.276, pp. 425-454.
- Turner, F.J. and Verhoogan, J. (1960) Igneous and Metamorphic Petrology. McGraw-Hill Book Company, Inc., Toronto, 694 pp. Appalachians. Canadian Journal of Earth Sciences, vol.18, pp. 386-394.
- Zentilli, M. and MacInnis, I. (1984) Stratigraphic Control and Metallogenesis, Meguma Terrane, Nova Scotia, Internal Report, Dalhousie University.

Appendix 1 : Trace Element Data For Granitoid (ppm)

Trace Element (ppm)	ZGB-0264	ZGB-0300	ZGB-0305	ZGB-0306
Ba	963	869	819	563
Rb	147	149	139	191
Sr	217	248	228	148
Y	30	29	21	17
Zr	232	259	263	155
Nb	14	16	15	11
Th	11	8	13	11
Pb	37	25	18	27
Ga	20	22	23	21
Zn	107	106	79	77
Cu	2	6	4	-1
Ni	10	8	8	8
TiO ₂ (wt. %)	0.84	0.93	0.94	0.52
V	51	73	69	33
Cr	22	26	25	27

Trace Element (ppm)	ZGB-0265	ZGB-0266	ZGB-0267	ZGB-0307	ZGB-0308
Ba	82	346	468	406	331
Rb	160	223	215	206	231
Sr	24	58	73	65	50
Y	7	8	8	9	6
Zr	17	68	60	71	71
Nb	11	8	9	9	8
Th	-1	7	6	6	7
Pb	19	24	31	31	22
Ga	22	21	19	17	23
Zn	27	50	46	52	35
Cu	-6	-5	-5	-4	-6
Ni	4	4	5	5	6
TiO ₂ (wt. %)	0.06	0.17	0.14	0.17	0.17
V	1	5	4	9	2
Cr	4	13	2	8	6

Appendix 2 Trace Element Data of Hole 26

Trace Element (ppm)	ZGB-1589	ZGB-1591	ZGB-1593	ZGB-1595	ZGB-1597
Ba	337	426	638	507	1132
Rb	47	63	74	59	139
Sr	215	188	202	166	76
Nb	10	12	13	11	17
Th	7	6	8	6	59
Pb	47	21	24	36	4041
Ga	9	10	16	15	16
Zn	110	56	53	73	9296
Cu	4	2	5	4	36
Ni	14	21	28	22	45
TiO ₂	0.59	0.63	0.74	0.69	0.96
V	60	69	84	82	128
Cr	273	288	256	244	170

Trace Element (ppm)	ZGB-1564	ZGB-1565	ZGB-1567	ZGB-1569	ZGB-1571
Ba	1012	943	719	408	839
Rb	287	205	144	69	186
Sr	162	272	228	149	183
Y	36	25	29	16	32
Zr	197	185	217	177	191
Nb	18	17	17	13	17
Th	168	171	61	84	118
Pb	13416	14108	4724	6310	9072
Ga	4	3	19	2	12
Zn	29486	31066	18007	11208	25891
Cu	109	52	42	22	81
Ni	50	56	18	18	47
TiO ₂	0.90	0.89	0.86	0.63	0.83
V	152	135	113	68	120
Cr	162	158	186	249	184

Trace Element (ppm)	ZGB-1573	ZGB-1575	ZGB-1577	ZGB-1579	ZGB-1581
Ba	904	925	862	790	821
Rb	194	189	173	158	135
Sr	205	212	209	228	198
Y	38	36	35	31	34
Zr	199	196	213	189	177
Nb	18	18	17	15	16
Th	109	105	118	123	14
Pb	8005	7823	9236	9694	107
Ga	13	12	11	8	27
Zn	17457	13158	20636	20258	172
Cu	42	44	42	55	27
Ni	31	28	37	38	48
TiO ₂	0.89	0.85	0.92	0.87	0.90
V	142	140	153	167	178
Cr	202	151	183	177	191

Trace Element (ppm)	ZGB-1598	ZGB-1600	ZGB-1583	ZGB-1585	ZGB-1587
Ba	835	767	859	941	911
Rb	145	142	128	145	156
Sr	207	192	214	215	216
Y	32	28	33	35	27
Zr	164	169	184	175	171
Nb	16	15	15	17	16
Th	12	16	29	31	104
Pb	65	495	1482	2013	7866
Ga	29	27	25	26	14
Zn	143	2298	4588	4260	20978
Cu	33	47	36	39	57
Ni	43	54	34	42	40
TiO ₂	0.90	0.90	0.89	0.86	0.79
V	204	182	144	167	172
Cr	194	180	198	192	182

Trace Element (ppm)	ZGB-1602	ZGB-1604	ZGB-1605	ZGB-1606	ZGB-1607
Ba	938	778	773	929	933
Rb	148	160	108	158	184
Sr	207	206	149	129	150
Y	31	38	30	31	32
Zr	151	183	126	125	129
Nb	16	17	18	18	19
Th	19	14	17	17	19
Pb	742	50	132	58	46
Ga	29	31	24	29	26
Zn	1952	395	350	137	120
Cu	37	31	37	39	34
Ni	48	38	52	49	46
TiO ₂	0.84	0.97	0.86	0.90	0.98
V	301	177	122	123	137
Cr	175	169	176	153	160

Appendix 3 : Whole Rock Major Element Analysis for Granitoid

Major Element (wt. %)	ZGB-0266	ZGB-0267	ZGB-0300	ZGB-0305	ZGB-0306
SiO ₂	72.38	72.98	63.93	64.56	64.28
Al ₂ O ₃	15.75	15.71	17.70	17.47	15.31
F ₂ O ₃	1.08	1.16	5.35	5.39	3.08
MgO	0.36	0.34	1.68	1.72	1.15
CaO	0.43	0.42	2.31	2.18	1.46
Na ₂ O	3.64	4.14	3.78	3.89	4.07
K ₂ O	5.63	4.48	3.55	3.28	3.91
TiO ₂	0.17	0.17	0.82	0.82	0.49
MnO	0.02	0.02	0.13	0.11	0.06
P ₂ O ₅	0.37	0.34	0.29	0.31	0.26
Total	99.82	99.76	99.56	99.73	94.07
L.O.I.	0.77	0.85	0.92	1.23	0.85

Major Element (wt. %)	ZGB-0307	ZGB-0308	ZGB-0264	ZGB-0265
SiO ₂	73.23	71.93	66.18	77.72
Al ₂ O ₃	15.71	15.51	16.30	14.56
Fe ₂ O ₃	1.19	1.11	4.84	0.73
MgO	0.41	0.33	1.55	0.21
CaO	0.45	0.38	2.04	0.31
Na ₂ O	4.00	3.89	3.51	3.67
K ₂ O	4.77	4.82	3.71	3.57
TiO ₂	0.18	0.19	0.82	0.08
MnO	0.03	0.02	0.12	0.02
P ₂ O ₅	0.34	0.36	0.32	0.34
Total	100.31	98.53	99.40	101.22
L.O.I.	0.85	0.85	0.69	0.77

Appendix 4 : Whole Rock Major Element Analysis of Hole 26

Major Element (wt. %)	ZGB-1589	ZGB-1591	ZGB-1593	ZGB-1595	ZGB-1598
SiO ₂	79.13	76.93	71.48	73.70	55.17
Al ₂ O ₃	9.81	11.20	14.01	13.52	21.81
Fe ₂ O ₃	2.81	3.43	4.69	3.96	8.51
MgO	0.98	1.31	1.81	1.54	2.01
CaO	1.00	0.85	1.02	0.65	0.28
Na ₂ O	2.71	2.51	2.71	3.15	1.00
K ₂ O	1.57	1.87	2.52	2.08	3.58
TiO ₂	0.54	0.57	0.65	0.62	1.01
MnO	0.08	0.08	0.12	0.11	0.14
P ₂ O ₅	0.11	0.12	0.14	0.14	0.14
Total	98.72	98.87	99.16	99.51	93.66
L.O.I.	1.00	1.23	1.77	1.54	6.62

Major Element (wt. %)	ZGB-1604	ZGB-1605	ZGB-1606	ZGB-1607
SiO ₂	56.53	59.71	59.88	59.49
Al ₂ O ₃	22.53	18.11	19.28	20.84
Fe ₂ O ₃	7.58	7.67	7.28	7.59
MgO	2.01	2.04	2.13	2.22
CaO	0.18	0.77	0.30	0.12
Na ₂ O	0.95	1.64	0.88	0.95
K ₂ O	3.81	2.71	3.66	3.90
TiO ₂	1.04	0.79	0.83	0.92
MnO	0.16	3.05	1.91	0.80
P ₂ O ₅	0.12	0.12	0.10	0.11
Total	94.71	96.61	96.24	96.91
L.O.I.	6.77	1.69	2.62	2.92

Major Element (wt. %)	ZGB-1564	ZGB-1565	ZGB-1567	ZGB-1569	ZGB-1571
SiO ₂	64.45	64.41	68.50	74.67	65.94
Al ₂ O ₃	24.18	23.35	19.78	14.52	22.37
FeO	3.36	4.47	4.65	4.77	4.79
MgO	2.05	1.86	1.76	1.64	1.73
CaO	0.18	0.98	0.93	0.57	0.89
Na ₂ O	0.26	1.18	1.70	1.19	0.81
K ₂ O	4.01	3.21	2.57	1.16	3.00
TiO ₂	1.08	0.98	0.93	0.57	0.89
MnO	0.22	0.04	0.15	0.27	0.13
Total	99.79	100.48	100.97	99.36	100.55

Major Element (wt. %)	ZGB-1573	ZGB-1575	ZGB-1577	ZGB-1579	ZGB-1583
SiO ₂	64.02	63.08	63.38	63.42	64.96
Al ₂ O ₃	24.22	24.75	23.89	26.40	24.06
FeO	4.82	5.57	5.33	2.84	4.39
MgO	1.68	1.79	1.85	1.79	1.80
CaO	0.33	0.33	0.60	0.42	0.63
Na ₂ O	0.74	0.57	1.01	0.97	1.02
K ₂ O	2.77	2.55	2.41	2.94	1.88
TiO ₂	0.91	0.89	0.98	1.05	1.04
MnO	0.31	0.28	0.17	0.02	--
Total	99.80	99.81	99.62	99.85	99.78

Major Element (wt. %)	ZGB-1585	ZGB-1587	ZGB-1597	ZGB-1600	ZGB-1602
SiO ₂	63.25	63.09	60.86	65.24	62.00
Al ₂ O ₃	25.70	25.48	19.02	23.71	25.96
FeO	2.77	4.01	8.66	5.21	4.54
MgO	1.91	1.99	3.34	1.67	1.83
CaO	0.44	0.33	0.75	0.41	0.32
Na ₂ O	1.29	1.11	1.21	0.59	1.04
K ₂ O	3.10	2.75	2.58	1.84	2.71
TiO ₂	1.09	1.03	0.84	1.00	1.06
MnO	0.04	--	2.25	0.08	0.02
Total	99.59	99.79	99.51	99.75	99.48

Appendix 5 : Drill Hole 26 Sample Location

<u>Sample Number</u>	<u>Strat. Interval</u> (m)	<u>Lithology</u>
1589	82.00-85.00	Quartzite
1591	88.00-91.00	Quartzite
1593	94.00-97.00	Quartzite
1595	100.00-103.00	Quartzite
1597	106.00-107.00	Quartzite
	Fault Zone	
1564	107.00-107.50	Slate
1565	107.50-107.90	Slate
1567	109.15-109.40	Slate
1569	110.70-111.10	Slate
1571	112.70-114.10	Slate
1573	115.60-116.90	Slate
1575	117.10-118.20	Slate
1577	118.55-120.00	Slate
1579	121.20-122.70	Slate
1598	128.00-131.00	Slate
1600	134.00-136.50	Slate
1583	138.50-140.50	Slate
1585	142.50-144.50	Slate
1587	146.50-148.50	Slate
1602	151.50-153.50	Slate
1604	156.50-159.50	Slate
1605	170.00-173.00	Schist
1606	173.00-176.00	Schist
1607	176.00-179.00	Schist